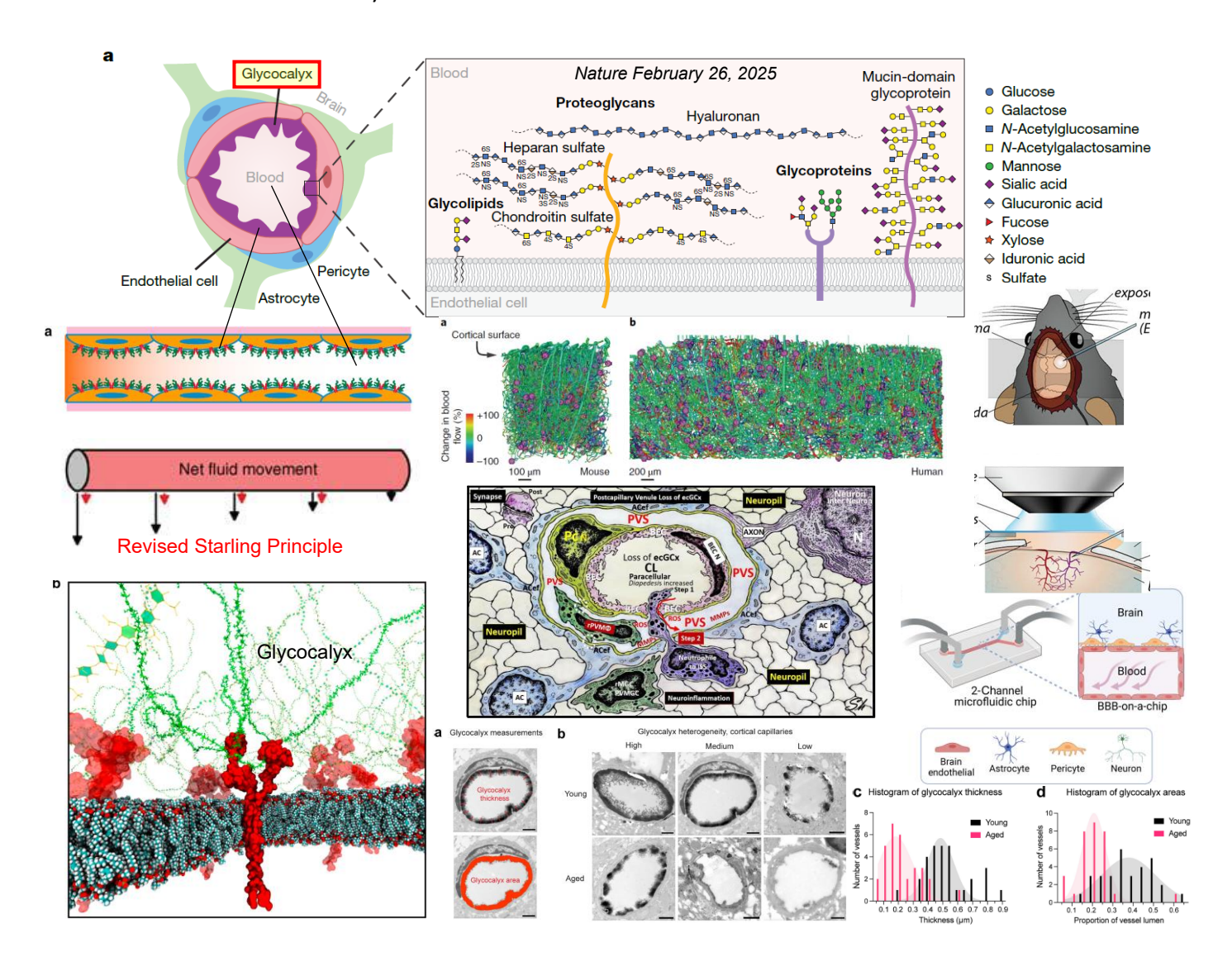
BRAIN ENDOTHELIAL GLYCOCALYX IN HEALTH AND DISEASE

Søren Andersen Master's Thesis Medicine*



Graphical Abstract prologue: Building on centennial discoveries from peripheral vessels discussed herein, recent research on a glycoprotein coating layer on endothelial cells (ECs) called the glycocalyx (GCX), turns out to be of importance both for the barrier properties of the blood-brain barrier (BBB) and for bidirectional signaling processes across the BBB to and from the brain. The BBB protects the brain from direct contact with the blood and consists of the GCX-coated ECs, pericytes and astrocytes. Through novel mechanistic *in vivo* studies, the GCX of the brain ECs is currently discovered as important for maintaining brain homeostasis throughout life. The GCX is possibly pivotal for preventing the common slowly progressing sporadic Alzheimer's disease and therefore a highly interesting candidate in the continued search for remedies to counter neurodegenerative diseases. (Figures mentioned on p. 11, 13, 19, 23, 29, 31, 32, 35, 40).

^{* ©} S. Andersen March 20, 2025. Presented April 23, 2025 at the Department of Neuroscience, Faculty of Health and Medical Sciences, University of Copenhagen, Denmark. S. Andersen is not an affiliate of the University of Copenhagen.

*Brain endothelial glycocalyx in health and disease (43 pp) © 2025 by Søren Andersen, DOI link https://doi.org/10.6084/m9.figshare.30391252 (47 pp total); licensed under CC BY-NC 4.0, to view a copy of this license, visit https://creativecommons.org/licenses/by-nc/4.0/. On-line October 18, 2025. Figures are under Copyright © and displayed here by non-exclusive permissions granted to S. Andersen by the listed (p. 46-47) Copyright © owners.

ABSTRACT

Glycocalyx (GCX) is a complex glycoprotein nanostructure resembling a dense bush in direct contact with the blood stream and that to variable extent covers the surface of endothelial cells (ECs), lining the inner surface of all arteries, veins and capillaries in the body. Its discovery has been a long time in the making because of its fragile and variable chemical composition and lack of adequate techniques to observe it. The last two decades have brought an explosion of knowledge on the GCX, bringing it from peripheral to frontier mainstream science of crucial importance to the understanding and treatment of vascular and neurodegenerative diseases. In all blood vessels, the negative charge and biophysical properties of the up to several micrometer long GCX, play an important role for the regulation of vessels' permeability to fluid and cells as well as ECs' NO production. In brain, the GCX is lately discovered to be an integral part of the NeuroVascular Unit (NVU) consisting of the ECs connected by tight junctions, pericytes and astrocytes. Synthesis of GCX by the ECs is complex and remains poorly understood; upon increased sheer-stress, more GCX appears on the EC surface. In brain capillaries, it constitutes a dense coating that in healthy vessels enmesh a large proportion of the vessel lumen. That the EC GCX shields the underlying tissue from immune cells like neutrophils binding to ICAM-1 surface receptors has been demonstrated both peripherally and recently now also in brain vessels; their infiltration induce inflammation and is thought to be a significant part of neurodegenerative disease etiology. Very recent research in mice, shows that natural thinning of the brain GCX with age correlates with a decrease in particularly a C1galt1p mucin-type O-glycan biosynthesis pathway enzyme, also found downregulated in human Alzheimer's disease, and that upregulation restores GCX thickness and cognitive abilities comparable to young mice. Research on the GCX is now entering a phase where it appears a realistic goal to find drugs targeting the GCX components, in the so far unsuccessful quest to find treatments for the rising incidents of neurodegenerative diseases, like in particular Alzheimer's disease, with its debilitating cognitive consequences for both individuals and society.

TABLE OF CONTENTS

1. INTRODUCTION

	1.1 The glycocalyx is a carbohydrate rich layer covering the surface of cells	3
	1.2 Formation and cellular constituents of the complex brain NeuroVascular Unit (NVU)	5
	1.3 Endothelial cells are connected by tight junctions and are the innermost vascular bed cells	s
	in the brain in direct contact with the blood stream	
	1.4 The glycocalyx covers the brain endothelial cells and is in direct contact with the blood	9
2.	FORMATION OF AND METHODS USED TO STUDY THE DYNAMIC GLYCOCALYX	
	2.1 Intracellular biosynthesis of the GCX	11
	2.2 Composition of the glycocalyx at the endothelial cell surface	13
	2.3 The interaction between the bloodstream, glycocalyx and the endothelial cells is dynamic.	
	2.4 Investigation of the glycocalyx entails a multifaceted approach	16
3.	EMERGENCE OF THE FUNCTIONS OF THE GLYCOCALYX AS A DYNAMIC COMPONENT OF	
	BLOOD VESSELS' ENDOTHELIAL CELLS	
	3.1 The revised Starling Principle: the surprising impact of the subglycocalyx space	
	3.2 The glycocalyx influences blood flow and is anywhere in the body an active component of	
	endothelial cells' signaling	
	3.3 The GCX can sense shear-stress and convert it to NO signaling and vascular tone	
	3.4 The glycocalyx is a component of the tripartite blood-brain barrier	
	3.5 The glycocalyx shields the endothelium and receptors and expose them when needed	26
4.	EXPERIMENTAL EVIDENCE FOR A ROLE OF THE GLYCOCALYX AS PART OF THE BLOOD-	28
_	POSSIBLE INVOLVEMENT OF GLYCOCALYX IN NEURODEGENERATIVE DISEASE ETIOLOGY.	
ວ.		
6	5.1 Glycocalyx' possible role in human Alzheimer's progression and treatment	
•-	SUPPORTING INFORMATION appendix	

1. INTRODUCTION

1.1 The glycocalyx is a carbohydrate rich layer covering the surface of cells

Before diving into this research essay, we need a short introduction to the word *glycocalyx*. Where it is located on cells and in the body? All eukaryotic cells are to some extent covered with carbohydrate on their outside surface. It may be attached to proteins in the cell membrane or coupled to lipids. All carbohydrates on glycoproteins, proteoglycans, and glycolipids are located on the outside of the plasma membrane (Fig. 1). This carbohydrate coating had been coined the constructed Greek word *glycocalyx* by Dr. Stanley Bennett in a seminar before the Mexican Anatomical Society in 1961 (Bennett (1963), p. 19). 'Glycocalyx' means 'sweet-husk' which, hence, is an extracellular carbohydrate rich structure on, possibly, most cells, bacteria and viruses.

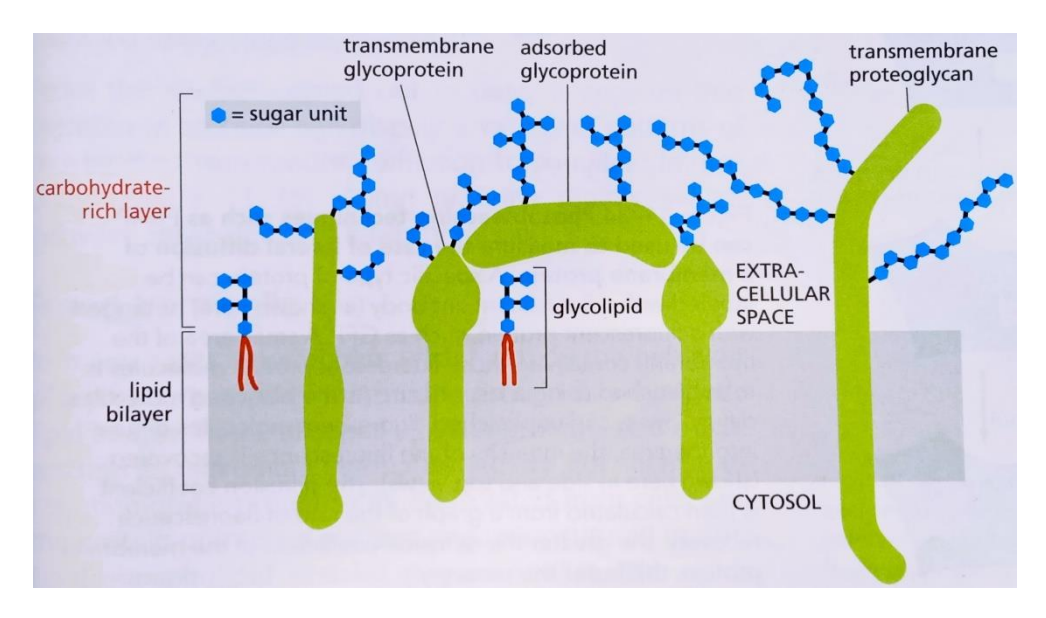


Figure 1. Eukaryotic cells are coated with sugars. This carbohydrate-rich layer is made of the oligosaccharide side chains attached to membrane glycolipids and glycoproteins, and of the polysaccharide chains on membrane proteoglycans. As shown, glycoproteins that have been secreted by the cell and then adsorbed back onto its surface can also contribute. Note that all the carbohydrate is on the external (noncytosolic) surface of the plasma membrane. (Adapted from Alberts et al. (2019), Fig. 11-33).

It is somewhat odd that carbohydrates do not seem as intensively studied as proteins and lipids. This possibly stems from lack of adequate techniques to study them, that they for example do not form enzymes with measurable enzymatic activity and often are elusive due to connections by rather unstable chemical bonds. We also mostly think of carbohydrates for their function as energy fuel for the body rather than as important cellular components. From immunology, however, there are many examples of carbohydrates serving as unique cell surface markers, providing essential immunological information concerning the origin of a given cell and whether it is self or non-self. A classic example in medicine is the AB0 blood group system, determined by minor changes in carbohydrate groups on the surface of the red blood cells, and knowledge of which is essential to avoid fatal blood coagulation upon blood transfusions in medical practice (Fig. 2, see legend p. 4 for details).

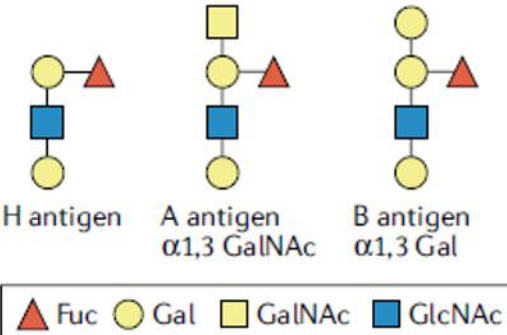
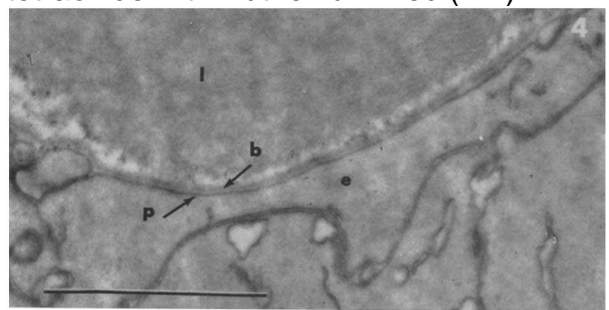


Figure 2. Many bloodare group antigens on erythrocytes are glycans conjugated to lipids or proteins. The AB0(H) blood-group antigens were discovered in the early 20th century based on the existence of antibodies in some individuals that agglutinated red blood cells from other individuals. These studies established, for the first time, that glycans can be antigenic and hence possess a three-dimensional structure which is also a very important theme in the study of glycocalyx functionalities. The AB0(H)-associated glycan epitopes are determined by the inheritance of glycosyltransferase genes in AB0, FUT1 and FUT2 loci. Group 0 individuals express the H antigen, the precursor to A and B antigens. Group A individuals have α1,3-N-acetylglucosamine (GalNAc) attached to the galactose residue of the H antigen, whereas Group B individuals have α1,3-Gal (Gal). Thus, one single sugar molecule group differs between the ABO(H) blood groups. Additional blood-group antigens have been described, and many contain glycan epitopes. (Adapted from Reily et al. (2019)).

Herein we shall use the term *glycocalyx* (GCX) to refer to the carbohydrate surface coating of the endothelial cells (ECs) that covers the inside of blood vessels. Yet, the GCX was not discovered in brain tissue vessels, and there are still only few studies available though there are many reviews available on the brain EC GCX. The Supporting Information appendix briefly discusses this issue (section 7.1, p. 39). Throughout, therefore, we have also to learn about GCX facts and functions by looking into research done on peripheral vessels' ECs.

Bennett's (1963) account shows and refers to EM photos of blood capillaries, taken around 1960 by Dr. Kiyoshi Hama (of Hiroshima University). Hence, labelling of the GCX marks a thin, delicate layer, which appears at the location of the basement membrane in rats but in invertebrate worms also on the surface facing the blood stream (Figure 3, left). At the time, these structures were difficult to reveal reproducibly - perhaps was due to different model systems and sample preparations. The first clear visualization of the EC GCX, in contact with and facing the blood stream, is therefore ascribed to (Luft, 1965) who replaced Osmium tetraoxide with Ruthenium Red (RR) in EM fixative and got a stronger staining (Fig. 3, right).



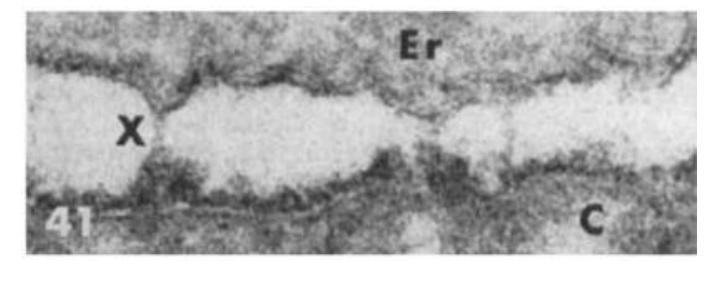


Figure 3: Left an EM photo of an earthworm blood capillary lumen stained without Ruthenium Red (RR); between the lumen (I, top) and the endothelial plasma membrane (p), is seen a different density (p) which is part of the GCX with a discernible narrow denser line 15Å thick (p points at this) and further towards the lumen (p) there is an unstained area (white); these are indications that there is some material between the plasma membrane and the lumen, namely the glycocalyx (GCX) (Adapted from figure 4 in Hama (1960), 50,000x magnification). [Legend continues on p. 5, top].

(Fig. 3 continued) *Right* is shown a mouse blood capillary stained with RR; an electron dense layer is seen on the surface of the capillary endothelial cell (*C*) facing the lumen. In the lumen is seen (some of) an erythrocyte (*Er*) floating; from its surface some electron dense material fans out and create some contact points (*X*) with the capillary endothelial surface layer. The electron dense layers from the Er and the C surfaces are defined as GCX. (Figure 41 from Luft (1971), the account from 1965 contains no images; 160,000x magnification).

Luft describes informatively: "There is morphological and physiological evidence for a layer of material possessing unusual and interesting properties lining the interior of blood vessels, and called the endocapillary layer [now called the 'glycocalyx', GCX] (Chambers and Zweifach, '47). However, its existence has been denied by most electron microscopists who looked for it, since little could be seen in its predicted location in electron micrographs. However, current EM techniques (aldehyde/osmium fixation in phosphate-type buffers, epoxy embedding and uranyl/lead staining) reveal a thin, delicate layer of material adherent to the outer leaflet of the luminal unit membrane of capillary endothelial cells. When the inorganic dye ruthenium red [RR] is added to the fixative, this layer is more easily seen. In typical capillaries from mouse diaphragm, the layer appears to be fluffy or flocculent and, although irregular, may be several hundred angstroms thick in places. It is continuous with the outer leaflet of the unit membrane and follows the membrane contours into the open pits or vesicles. The layer is not a basement membrane but is similar to the "fuzz" coating of intestinal microvilli and to the extraneous coats of amebae. Its enhancement by ruthenium red suggests that it contains polysaccharide substituted with many acidic groups (carboxylic or sulfuric) and that it may be an acid mucoprotein." (Luft, 1965).

Ever since Hama's, Bennett's and Luft's works, scientists have struggled to get better images of the GCX, first by EM and later, as we shall see, by light microscopy, with the purpose of gaining a better understanding of its possible functions. The 'glycocalyx' has now developed into a mature field of its own that is intensely investigated both from basic and applied scientific viewpoints, and research initiatives where the topic is involved, carry catchy names such as glycobiology, glycomics, glycoengineering and/or glycomedicine.

1.2 Formation and cellular constituents of the complex brain NeuroVascular Unit (NVU)

The inside of arteries and veins, i.e. all blood vessels, are lined with ECs. Figure 4 shows the vascular architecture of capillaries observed in brain (left), heart and kidney. As seen,

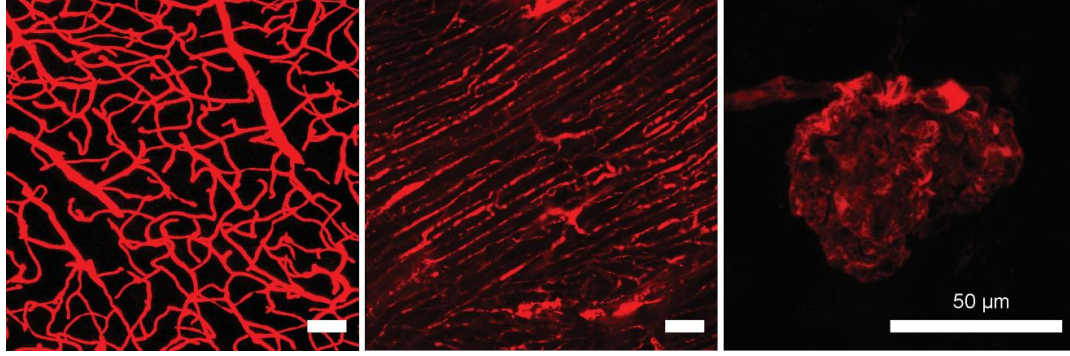


Figure 4. Variability in vessel morphology and function. Differences in vessel bed morphology, induced by organ-specific patterning, are easily discernible. *Left to right*: vessels of the adult mouse cerebral cortex show a tree-like pattern that maximizes blood flow to all of the cells in the brain; vessels of the adult mouse heart are organized in a manner that aligns with the cardiomyocytes; finally, vessels in the adult mouse kidney show a convoluted vascular structure. (Adapted from Udan et al. (2013)).

there are clear macroscopic differences stemming from the nutrient requirement, functions and cytoarchitecture of the various tissues.

Figure 5 (left) shows the dense arterial network in the human brain. Now, going from inside a microvascular vessel lumen and outwards (Figure 5, right), we have the apical endothelial cell side facing the lumen of the vessel with the GCX outermost in direct contact with the lumen. Their basolateral side is positioned on the basal/basement membrane that is secreted and shared by both the ECs astrocytes. Then there may be various 'mural cells' present on the surface of the ECs, namely smooth muscle cells and pericytes. The term 'mural cell' covers both pericytes and smooth muscle cells. The number, distribution and organization of mural cells depend on the type of vessel and tissue and is still subject to intense research. This illustration (Figure 5, right) schematizes the so-called 'NeuroVascular Unit' (NVU) of the brain's microvasculature as well as the cellular components forming the important Blood-Brain Barrier (BBB; see also Fig. 7-8).

The BBB functions to ensheath the capillary lumen and regulates transport tightly across the capillary wall. The key characteristic of the NVU microvasculature, compared with other vascular beds, is that the ECs are connected by tight junctions (TJ), which render this capillary wall almost impermeable to paracellular transport. Hereto comes that the GCX seems to be more prominent, or thicker, on the NVU capillary ECs than elsewhere in the vascular system, which adds to the BBB's impermeability, as we shall later see in more details.

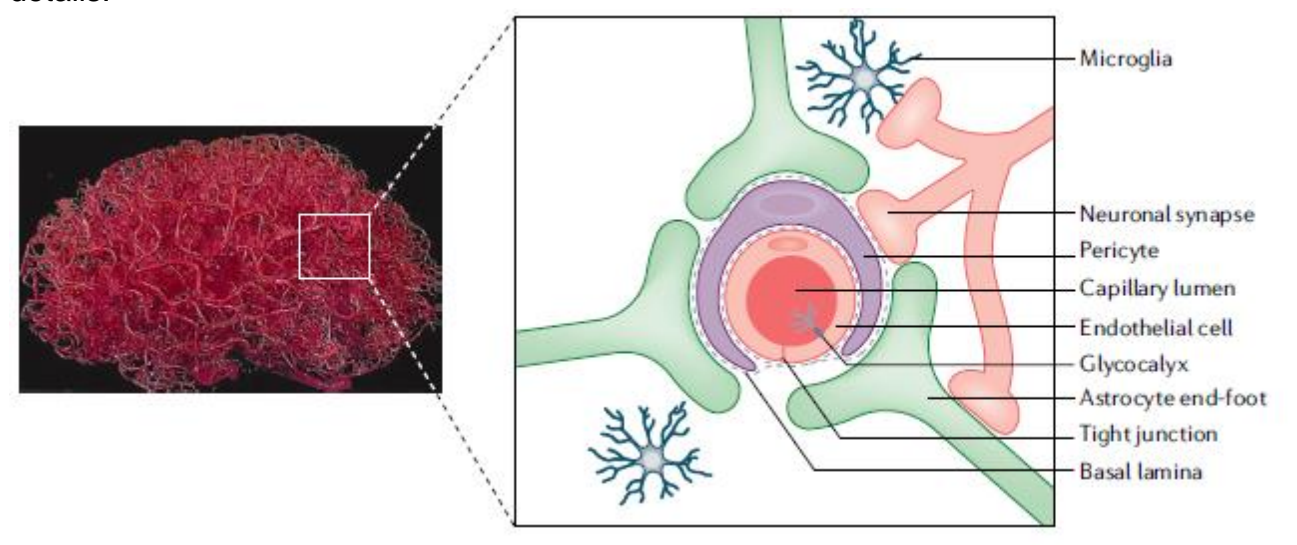


Figure 5. *Left*, the dense vascular network throughout the human brain (left panel) includes large-diameter arterioles wrapped in vascular smooth muscle cells, which branch into the microvasculature (known as the neurovascular unit (NVU); right panel) and then converge to venules (not shown). *Right*, the neurovascular unit (NVU) is composed of a single endothelial cell layer that is lined with brush-like glyocoproteins (glycocalyx/GCX) and tightly tethered together via tight junction protein connections. The endothelial cells are covered by a continuous basal lamina extracellular matrix membrane, pericytes and astrocyte end-foot processes. Innervation of neuronal synapses and neighbouring microglial cells (and other immune cells, not shown) complete the neurovascular unit (NVU). The structural components and dynamic cellular interactions are essential to the development and maintenance of the blood—brain barrier (BBB). (Adapted from Terstappen et al. (2021)).

Although only pericytes, and no smooth muscle cells (SMC), are shown in the schematic (Fig. 5, right), this depends on the anatomical location and remains a matter of debate of importance to vasomotor control and hence microvascular blood flow regulation (Hajal et

al., 2021). Moreover, some researchers define capillaries as vessels that are below 10 μm in diameter in rat brain and that are also lacking a continuous layer of SMC (Hall et al., 2014). That same study shows that pericytes extend processes along vessels' capillary diameter. The study goes on to show that pericytes are located closest to neurons and are the first to relax, upon neuronal activity, whereby capillaries dilate and then, further downstream of this, dilation of SMC around arterioles permit increased blood flow (Hall et al., 2014).

Understanding pericytes has long been and remains an active research field. Indeed, according to historical data by Bjovulf Jensen Vimtrup, published in 1922 and summarized by August Krogh (Krogh, 1929), these *Rouget cells* -- (Vimtrup named them after studies by Charles-Marie Benjamin Rouget from 1873; they were later renamed *pericytes* in e.g. studies by Zimmermann from 1923) -- Vimptrup observed (Fig. 6, his drawing), both in live capillaries and by methylene blue staining, appeared distinct compared to SMC, had contractile properties and could also contract in response to stimulation of nerves in the web of a small frog (Krogh (1929), p. 72-80).

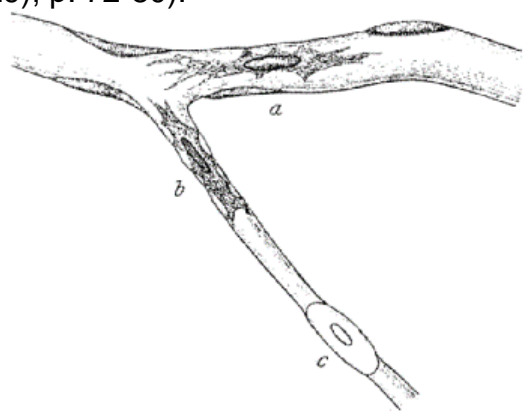


Figure 6. Two Rouget cells (*a* and *b*; called pericytes today) as seen on capillaries in living newt larvae, where *b* is contracting, *c* is a red blood cell. x500. (Adapted from Vimptrup (1922), Plate II, Figure 5).

Hence, from this it appeared pericytes had contractile properties of their own, independently of the SMCs (other experts confirmed this). Though, Krogh points out:..." it must be admitted that there are still a number of obscure points with regard to pericapillary cells and that some confusion is inevitable so long as no reliable methods have been elaborated by which the different kinds of such cells can be definitely distinguished." (Krogh (1929), p. 82).

Today, there are molecular markers for pericytes and the pericapillary cells remain a very active research field, not just in brain (Longden et al., 2023).

1.3. Endothelial cells are connected by tight junctions and are the innermost vascular bed cells in the brain in direct contact with the blood stream

We continue this introduction with a schematic cartoon of the NVU blood capillary with the all-important blood-brain barrier (BBB) and its five components: glycocalyx, endothelial cells connected with tight junctions, basement membrane, pericytes and astrocytes (Fig. 7-8). In recent years it has become increasingly clear that the GCX is an integral part of the BBB, as schematized in Figure 7-8, both as a kind of mechanical filter, negatively charged surface, and as an active component that transduces signals from the blood stream through the BBB to neuronal and glial cells in the brain.

In Figure 8, it is further illustrated how the five components of the BBB effectively shields the cells in the brain from direct contact with the blood stream.

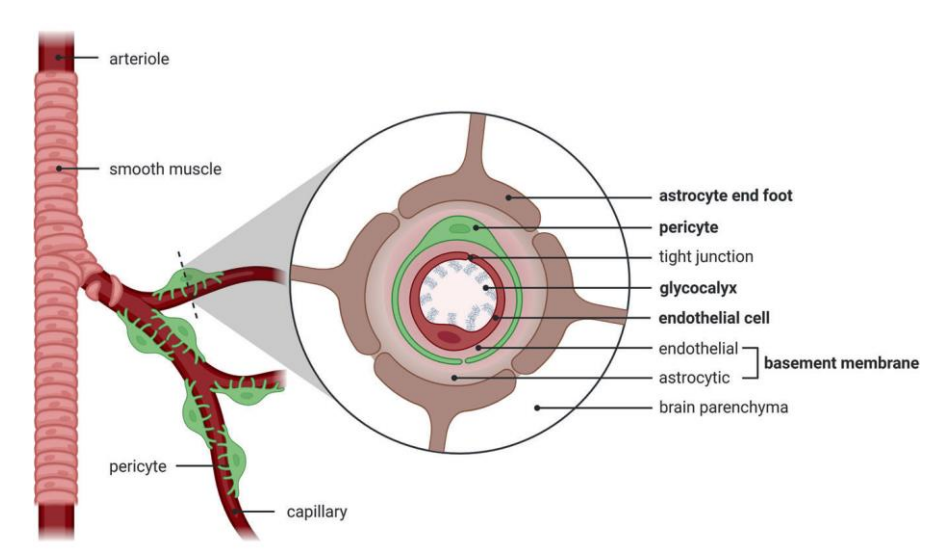
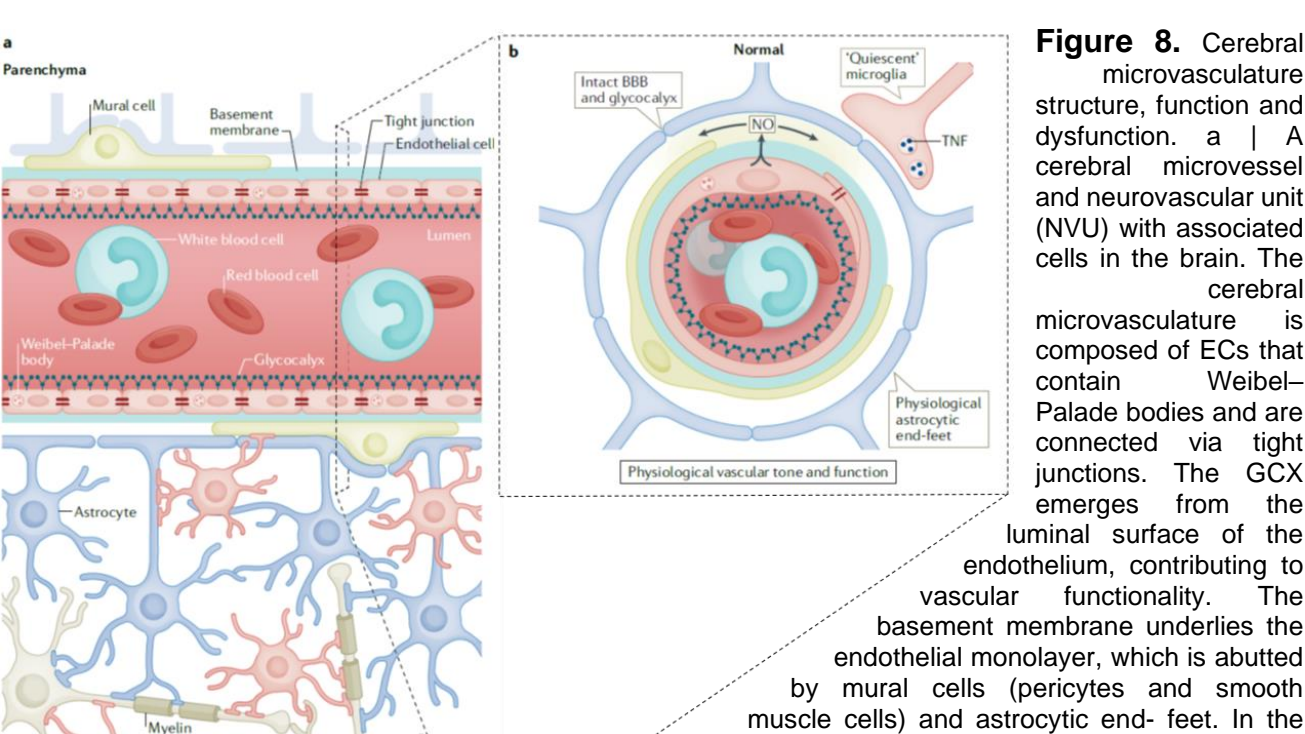


Figure 7. Vascular BBB. Alternating layers of molecular (GCX, basement membrane) and cellular (ECs, pericytes, astrocytes) components form the BBB. The five components are in bold typeface. The basement membrane is a single with a two-laver structure composition, since it is secreted endothelial cells astrocytes on either side. The tight iunctions prevent paracellular transport and are a hallmark property of the BBB. (Adapted from Galea (2021)).



Microglia

microvasculature structure, function and dysfunction, a | A cerebral microvessel and neurovascular unit (NVU) with associated cells in the brain. The cerebral microvasculature is composed of ECs that contain Weibel-Palade bodies and are connected via tight junctions. The GCX emerges from the luminal surface of the endothelium, contributing to

functionality. The basement membrane underlies the endothelial monolayer, which is abutted by mural cells (pericytes and smooth muscle cells) and astrocytic end- feet. In the parenchyma, astrocytes, microglia and neurons are intricately interconnected with multiple points of cellular communication. Oligodendrocytes are not depicted, b | Key cellular interactions under normal physiological conditions

where ECs produce the vasodilator nitric oxide (NO), which maintains normal vascular tone and helps facilitate blood flow. The luminal surface of the EC normally maintains a non- thrombotic and non- inflammatory environment, preventing adherent interactions with white blood cells or other blood cells. The GCX and BBB are structurally intact, protecting the brain from extravasation of blood components. Adjacent to the astrocytic end- feet are 'quiescent' microglia with processes that constantly survey the environment to assess and maintain homeostasis. (Adapted from Daniele et al. (2021)).

1.4 The glycocalyx covers the brain endothelial cells and is in direct contact with the blood

Following Hama, Bennett and Luft, there is now agreement that a GCX covers the surface of the ECs that are lining the innermost part of the blood vessels in the brain and elsewhere in the body. However, its distribution, organization, density, dynamics and precise chemical formulation remain topics that are intensely investigated and debated. Important research remains imaging of the GCX, and *in vivo* 2-photon microscopy was applied previously to reveal the GCX on ECs of the carotid arteries in mice. GCX showed an EC coverage of around 60-70 % (Megens et al., 2007; van Zandvoort et al., 2004). The first *in vivo* 2-photon study of cerebral GCX showed likewise that the coverage was not complete (Yoon et al., 2017). Interestingly, the latter study could not detect GCX in veins (using WGA-FITC) and they speculate this may be because vascular tone is not regulated on the venous side to the same extent as on the arterial side (Yoon et al., 2017), and as the GCX is found implicated in NO-regulated vascular tone, as we shall later see in more detail. Yet, later 2-photon studies have observed GCX in brain venules (Kucharz et al., 2022b) although less abundant than in arterioles .

Indeed, just getting nice images of GCX on the ECs of a blood vessels remain publishable material. This is in part due to the ephemeral and fragile nature of the GCX rendering imaging difficult and prompting continuous improvement of techniques and imaging methods. An example is shown in Figure 9 (Ando et al., 2018), where a blood capillary from a mouse brain has been stained with Lanthanum (La3+) nitrate (LAN) and viewed by scanning EM, rendering some superb images of the GCX (Fig. 9 A). However, though endothelial cells seem completely covered with GCX, this may be an artefact. Hence, La3+ also binds Ca²⁺ binding sites, wherefore this type of study does not permit drawing quantitative conclusions. Nevertheless, (Ando et al., 2018) quantifies by transmission EM that the percentage area covered by GCX in brain capillaries, around 40%, is significantly higher than in the lung, heart tissues studied (Fig. 9 B). Because this concerns the same technique, by the same group within the same study, this quantification can be used reliably to conclude that, relatively speaking, most likely there is more GCX in brain capillaries than elsewhere. However, if a different technique is used, and even if just performed in another laboratory, the absolute differences very likely will be different. To illustrate this, in a simultaneous study, (Kutuzov et al., 2018) used Wheat Germ Agglutinin (WGA) coupled to the red fluorescent dye Alexa to label the GCX in rat brain capillaries, WGA-Alexa (Fig. 9 C). We see from this a red circle demarcating the inside of the lumen of the brain capillary that stains with WGA-Alexa and hence is the signal of the GCX. It seems to be a homogenous red staining, and hence a homogenous and full coverage of the endothelial surface by GCX. However, this cannot be concluded from this, as emanating light from the fluorescent probes is spread and diffracted and does not provide a resolution to determine how the GCX is distributed on the surface. Moreover, there may be significant biological variations both in GCX density and coverage that escape detection when using a fluorescent probe like WGA-Alexa that preferentially binds heparan sulphate. We shall return to the study by (Kutuzov et al., 2018) later because it addresses the GCX as part of the BBB. Here it is shown to illustrate another way to reveal the presence of the GCX at the lumen of the brain EC capillaries as compared to that of (Ando et al., 2018).

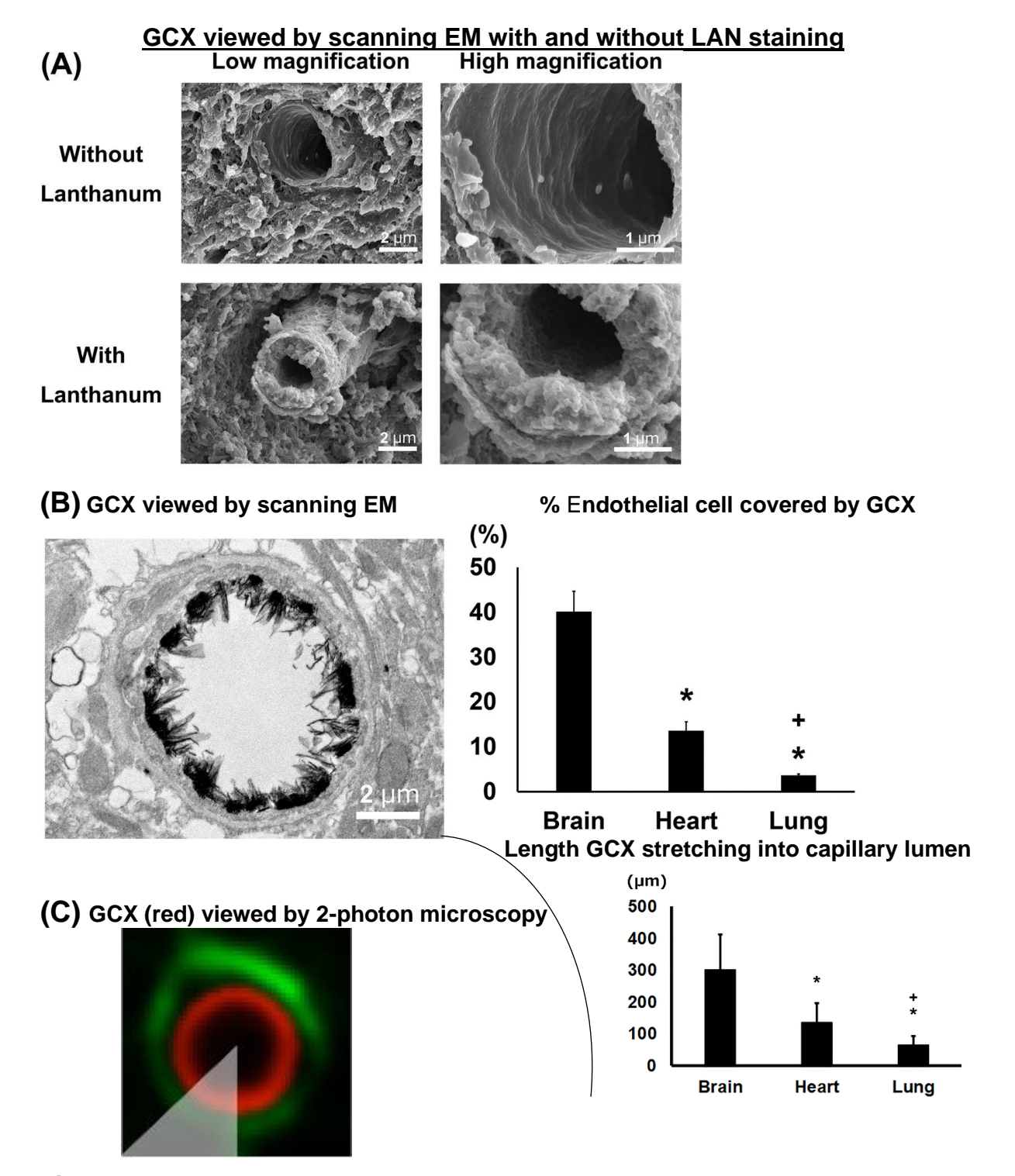


Figure 9. (A), Scanning electron micrographs showing the ultrastructure of continuous capillaries in the brain of mouse with and without LAN staining. (Adapted from Ando et al. (2018)).

(B), *left*, transmission electron microscopic analysis of continuous brain mouse capillaries; *right*, *(top)* quantified percent area covered by endothelial GCX in brain capillaries and heart and lung (images not shown in the paper); *(bottom)* length of the stained GCX emanating into the lumen in the image shown on the left. Bars indicate means \pm SE. *p < 0.05 vs brain (adapted from (Ando et al., 2018)).

(C), The lumen of the capillary is in the center of the picture (appears *black*), and the *glycocalyx* (*red*) and *astrocyte endfeet* (*green*) were labeled with WGA-Alexa and SR101, respectively (adapted from Kutuzov et al. (2018); we return to this later in Figure 16A, p. 24).

That GCX is part of the BBB had already been described and thought for several decades but the Kutuzov et al. (2018) study provides quantitative *in vivo* measurements of this fact. As illustrated, the most remarkable is perhaps that the GCX takes up and projects into such a large portion of the lumen of blood capillaries in general and in particular in the brain (Fig. 9B; also illustrated in the Graphical Abstract, bottom). This is in stark contrast to the view held at the time of Hama, Bennett and Luft, where the GCX was thought to be a rather flat coating on the ECs. In the next section we shall look closer at the constituents of the GCX.

2. FORMATION OF AND METHODS USED TO STUDY THE DYNAMIC GLYCOCALYX

2.1 Intracellular biosynthesis of the GCX

In overview, the GCX consists schematically of two major parts, as illustrated in Fig. 1, with one part anchored to the endothelial plasma membrane and another part consisting of molecules from the blood stream that continuously attaches non-covalently to and detaches from the GCX. The GCX is hence a dynamic structure continuously changing in composition.

The membrane-attached part of the GCX is synthesized by the ECs. It is hence genetically encoded by the ECs and subject to regulation. Study of these processes is difficult owing to the fragile nature of the GCX components and regulation of synthesis by both intracellular and extracellular factors. Therefore, it has not yet been possible to write up a pathway that sets in stone what the GCX presented on the ECs precisely looks like. Its synthesis is a dynamic process that most likely also encompass some randomness as those seen in non-linear chaotic systems.

What is clear is that even though the GCX contains a common core - of proteoglycans (PG) with both non- and covalently attached glycosaminoglycans (GAG) - there are differences in the GCX composition on the ECs throughout the body, and these differences are subject to intense research. For example, if it were possible to regulate the GCX composition, that change could perhaps be used as part of drug therapies to modify permeability of the BBB to treat diseases and conditions.

Therefore, we delve somewhat on the synthesis of the GCX as shown in Figure 10 (p. 12). The GCX of the ECs contains proteoglycans (PG) such as Syndecan-1 and Glypican-1 with covalently attached glycosaminoglycans (GAG) such as Heparan and Chondroitin. Both of these are sulphated to variable degrees, which provides the GCX with its characteristic and functionally important negative surface charge.

To make the GCX, at first a *core protein* is synthesized on the endoplasmatic reticulum (ER) and either inserted into the ER membrane as a single spanning protein (ie. Syndecan-1), or upon its synthesis released into the ER and later attached to a membrane leaflet through a Glycosylphosphatidylinositol (GPI) linker (ie. Glypican-1).

The core protein is a substrate for a xylosyltransferase in the ER lumen that transfers UDP-xylose (UDP-Xyl) to the OH group of a specific Serine residue in the core protein (Figure 10 A, from Ballinger et al. (2004)). This xylosylated core protein is then transported to the cis-Golgi where two galactose groups are enzymatically transferred, followed by a glucuronic acid group (GlcA). Now then this *glycan linker* is attached to the *core protein*, forming the nascent ProteoGlycan (PG): core protein-Serine-Xyl-Gal-Gal-GlcA; this is subsequently modified enzymatically by sequential addition of glucosamine and Heparan Sulphate (HS) and/or Chondroitin sulphate (CS) groups forming the glycosaminoglycan (GAG) polymer. In Syndecan-1 is found both HS and CS whereas in Glypican-1 is found only HS. Both are therefore known as HS PGs.

After chain polymerization the GAG chain undergoes further covalent modification through both N- and O- linked sulphation. These elongation and modification reactions take place in the cis- and trans Golgi networks. These processes are illustrated in Figure 10B (p. 13) that also displays the enzymatic steps involved and the symbolic used in the field to annotate specific sugar molecules (adapted from Milusev et al. (2022)). Through regulated vesicular transport, the Syndecan-1 and Glypican-1 are then presented on the plasma membrane as part of the GCX. Hence, these steps require a number of different enzymes and are subject to various types of intrinsic regulation by the ECs, which however remain poorly understood and studied. From this it transpires that ways to modify GCX synthesis and composition include at least: limited availability of specific building blocks, direct regulation of enzyme activity and regulation of vesicular transport.

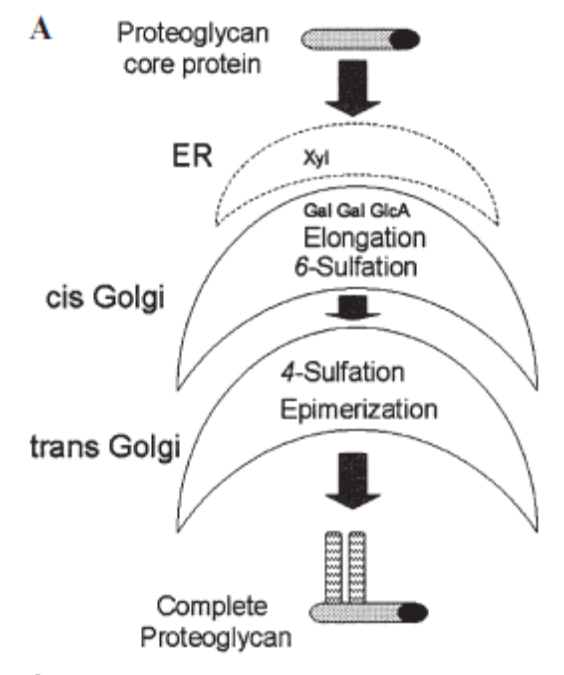
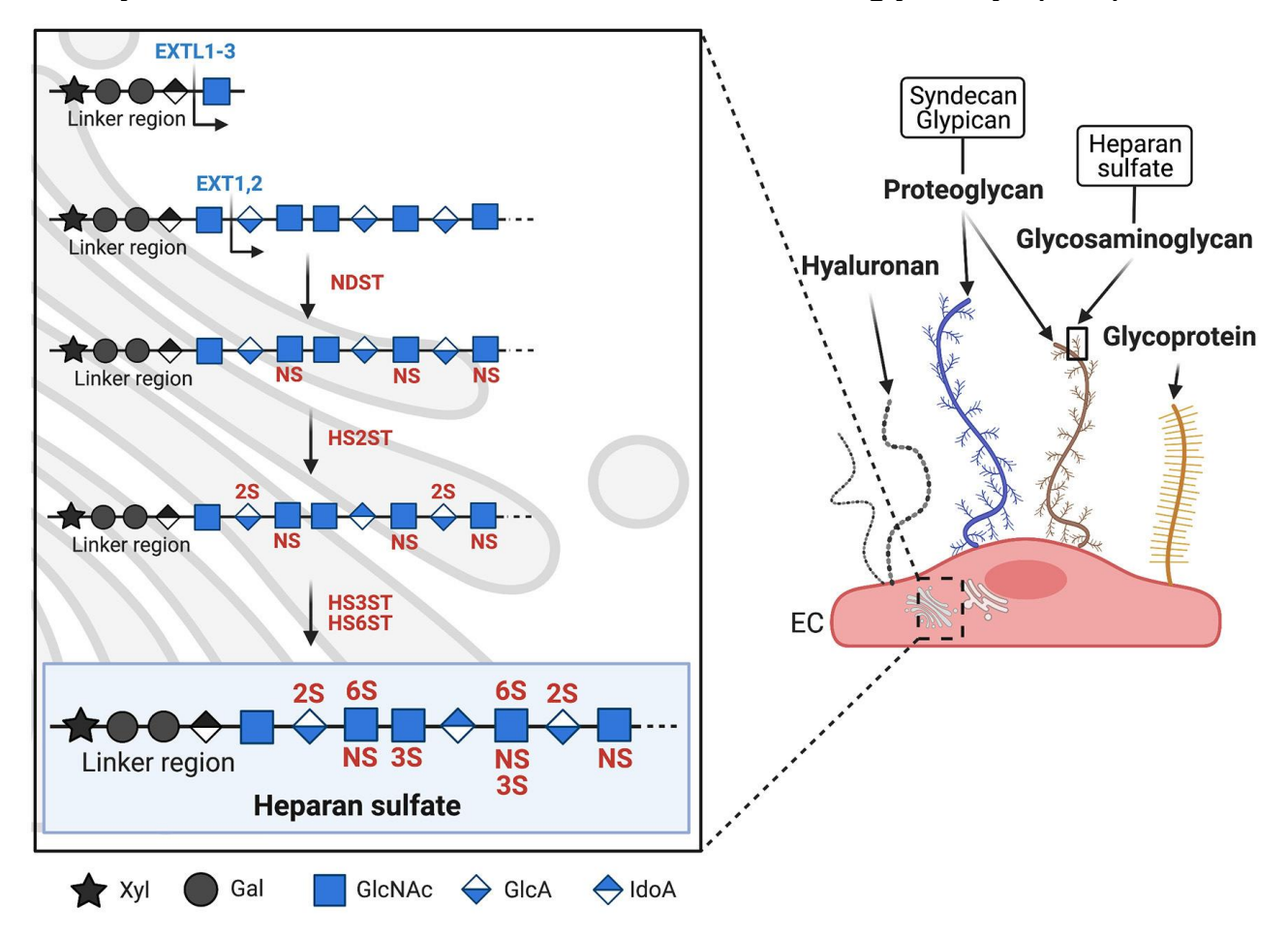


Figure 10. (A) Schematic of synthesis of a proteoglycan (PG) like Syndapin-1 and Glypican-1, from core protein through the ER-Golgi to the PG ready for presentation at the EC surface. See text p. 11 for details. (Adapted from Ballinger et al. (2004)).

(B, on p. 13, top) Biosynthesis and structure of the endothelial glycocalyx. Schematic representation of the major GCX components covering the luminal surface of microvascular endothelial cells (EC). On the right panel, syndecan (blue) and glypican (brown) are shown as two examples of proteoglycans (PGs). PGs carry long glycosaminoglycan (GAGs) side chains, while other glycoproteins (shown in yellow) carry shorter, unbranched carbohydrate side chains. The left panel shows the biosynthesis of heparan sulfate (HS), the major GAG expressed on EC. HS biosynthesis takes place in the Golgi apparatus and is mediated by different enzymes. Synthesis is initiated by the enzyme EXTL1-3 which adds the first sugar to the linker region. Chain elongation is performed by EXT1-2 which add GlcNAc and GlcA. Sulfotransferases then initiate HS sulfation, starting with NDST which sulfates GlcNAc at the N-acetyl position. HS2ST sulfates uronic acid, HS3ST and HS6ST finish sulfation by adding sulfate respectively to the 3-O and 6-O position of GlcNAc. Xyl, xylose; Gal, galactose; GlcNAc, N-acetylglucosamine; GlcA, glucuronic acid; IdoA, iduronic acid; NS, N-sulfation; 2S, 2-O sulfation; 3S, 3-O sulfation; 6S, 6-O sulfation; EXTL, exostosin-like glycosyltransferase; NDST, N-deacetylase/N-sulfotransferase; HS2ST, HS 2O-sulfotransferase; HS3ST, HS 3O-sulfotransferase; HS6ST, HS 6O-sulfotransferase. (Adapted from Milusev et al. (2022)).

B Biosynthesis and chemical structure of the endothelial glycocalyx (GCX)



2.2 Composition of the glycocalyx at the endothelial cell surface

In the previous section we briefly looked into the synthesis of the GCX. Full understanding of this area is essential to progress further on the attempts to modify and/or use the GCX therapeutically in disease management and as a gate-way to cross the BBB. However, it appears there is still some way to go before that goal is within reach.

Through various model-drawings depicting the GCX, we shall here look further at the GCX in qualitative terms to get a better understanding of its 3D organization and molecular composition, and in later sections return in more detail to effects of this organization.

Figure 11A (p. 14) shows key constituents of the dense GCX layer which covers the ECs. Importantly, surface receptors, such as for signaling and adhesion (named *glycoprotein* in the figure), stick only 10-20 nm out in the lumen from the EC membrane whereas the GCX may project several hundred micrometers into the lumen (see Fig. 9B; the Graphical Abstract depicts similar data). In addition, the GCX carries a net negative charge owing especially to many sulphate groups. Consequently, the surface receptors are shielded from luminal content beyond a certain size and charge. For example, erythrocytes are negatively charged and of a size that completely excluded them from the EC surface (as also seen by Luft in Figure 3); the abundant blood protein Albumin is also negatively charged and has a molecular weight of around 70 kDa. Because of the GCX density and negative charge, Albumin is therefore also excluded efficiently from direct interaction with the EC surface. CD44 is a receptor for the negatively charged hyaluronic acid polymer (HA). HA can have

molecular weights over 500 kDa. Three membrane-bound synthases make HA at the inner surface of the EC membranes, and the growing polymer is extruded to the lumen where it binds the CD44 receptor. Syndecan-1 has a single integral transmembrane spanning region and is involved with regulation of the actin cytoskeleton. Glypican-1 is attached by a glycosylphosphatidylinositol (GPI) linker and part of membrane rafts and likely involved with shear-stress sensing from flow in the vessel. Figure 11B (p.15) provides the same information as Fig. 11 (A) and provides in addition a qualitative illustration of the *higher density of the GCX layer in the brain microvasculature* (right) compared with the peripheral vasculature (left). Figure 12 and figure legend are supplementary (see Supporting Information appendix, section 7.2, p. 40) and give an additional even more detailed cartoon of the GCX composition and organization whereof some are addressed at later points.

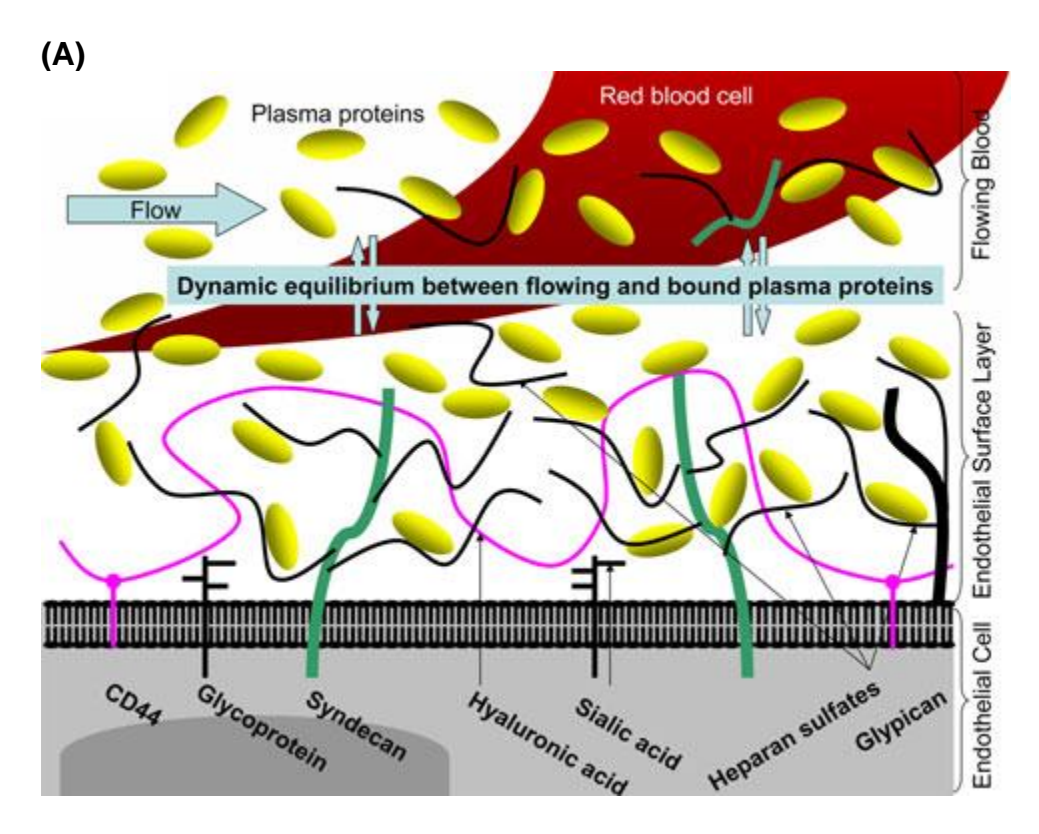


Figure 11. (A) Schematic arrangement of the chief constituents of the endothelial GCX and the established endothelial surface layer. Glycoproteins include intercellular and vascular adhesion molecules, selectins and integrins. These all extend at most 10–20 nm from the lipid double layer and are, consequently, normally sequestered beneath a healthy [GCX] surface layer. Shed components of the GCX are to be found in normal plasma. CD44 is a membrane receptor non-covalently binding, as the only GAG in the GCX, the negatively charged GAG hyaluronic acid (HA). (Adapted from Becker et al. (2010)).

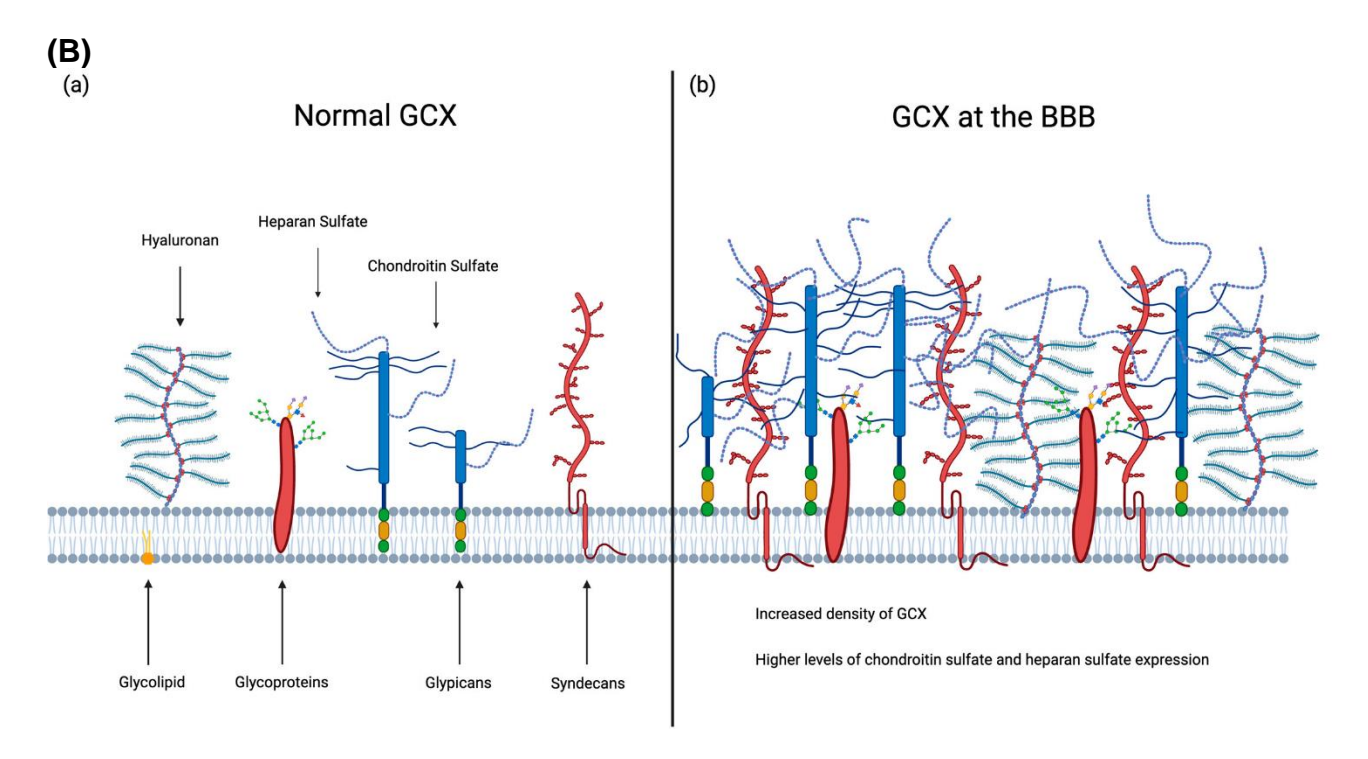


Figure 11. (**B**) A representative comparison of the vascular GCX in the periphery and lining the interior cerebrovasculature at the BBB. (**a**) The mesh-layer of polysaccharides within a normal endothelial GCX includes, from left to right, glycolipids, hyaluronan (HA) with aggrecan containing brushes, glycoproteins, heparan sulfate (HS) (blue and purple chain) and chondroitin sulfate (solid blue chain) attached to syndecans, and glypicans. (**b**) The endothelial GCX at the BBB contains the same major components as the peripheral GCX (shown in (a)) but exhibits a higher density, with notably higher levels of chondroitin sulfate and HS expression; these function to stabilize and enmesh GCX components. (Adapted from Dancy et al. (2024)).

2.3 The interaction between the bloodstream, glycocalyx and the endothelial cells is dynamic

In previous sections, we have seen that the blood stream with erythrocytes, immune cells, proteins, enzymes, lipids, salts and so forth interacts with and influences the GCX, that the GCX therefore impacts back on the blood stream, and the GCX through the plasma membrane influences the EC that in turn regulate expression of the GCX and other molecules through genetic regulation. These three different compartments, or tripartite constellation, of 1) the blood stream, 2) the GCX and 3) the EC make it impossible to predict with certainty the structure and components of the GCX at a given time. The structure at any given time develops as a chaotic stochastic process. An analogous principle is known from quantum physics, as in Helium with its one nucleus and two electrons, which owing to the three-body problem cannot be solved exactly but where it is necessary to use quantum physics to make a description of the position of the electrons, introducing uncertainty and stochasticity characteristic of modern physics compared to classical physics.

It appears that a very important consequence of the tripartite constellation of the GCX is that it is not possible to draw a lot of conclusions from studies that only studies part of the system. For example, in *in vitro* experiments, where ECs are grown on a substrate, subjected to some factor that binds a receptor on the cells and an outcome is monitored. In this example, flow and shear stress is missing from the system as well as all the components present in the blood stream constantly racing by. Therefore, study of the GCX needs to be done under conditions that are as much *in vivo*-like as possible. Indeed, a number of

experimental systems have been invented where flow and shear stress is added to an *in vitro* system (reviewed in Deli et al. (2024) and O'Hare et al. (2024)). Application of two-photon microscopy has rendered it possible to look at the GCX in real time *in vivo*, not just fixed EM, although the resolution of such studies remains limited to the few submicrometer scale (λ /2), owing to the wavelength (λ) of light used. In the next section, we shall make a brief overview of techniques used to study the GCX.

2.4 Investigation of the glycocalyx entails a multifaceted approach

In the attempt at getting to understand the GCX, many techniques are used. We shall not present them here in any detail but refer the reader to available literature. Listing them encompass at least: electrophoretic 1- and 2D gels, mass spectroscopy and omics methods; various microscopy methods such EM, confocal, two-photon and more rare such as sidestream dark field (SDF) imaging of brain microcirculation following cranioectomy (Haeren et al., 2018) and *in vitro* atomic force microscopy experiments, MRI is not used but may be developed and is currently used to try assess BBB permeability *in vivo* (Leaston et al., 2021); genetics and molecular gene manipulation; cellular *in vitro* studies and microfluidics technology; study of GCX components shed into blood *in vivo* as disease marker; epidemiological and postmortem data; data mining and analysis of *existing* bulk RNA-sequencing dataset of brain endothelial cells from young (3 months) and aged (19 months) mice searching for changes in glycosylation-related genes with age (Shi et al., 2025); specific upregulation and downregulation of glycosylation-related genes in brain ECs *in vivo* through infection with a brain ECs specific adenovirus vector; EC flowcytometry and microvessel purifications and antibody staining for various glycosylations (Shi et al., 2025).

All these techniques, highlighted by the very exciting very recent Shi et al. (2025) paper, illustrate that the field demands very advanced techniques to investigate potentially novel aspects, and that only very few laboratories in the world can afford and have access to. Moreover, an important point is that with so many different sources of information, there will be discrepancies and disagreements between results, and notably conclusions, that are trying to investigate the same questions. One example is the thickness or length of this nanogel that the GCX constitutes, which depends very much on the technique used, as mentioned (Fig. 9). Also, it illustrates how difficult it is to study this GCX layer and its dynamics. It is constantly changing, and subtle changes are likely of functional importance. A technique of interest to mention is old-fashioned purification of ECs, from where it is possible to study the GCX. In Ghitescu and Robert (2002) they purify the luminal part of ECs from lung, heart and brain and compare their GCX by gel electrophoresis and western blotting and stain with different lectins. The purification is done by perfusing cationic colloid silica nanoparticles into the vessels that then bind the negatively charged GCX. Because of the density of the particles, they can be isolated by centrifugation, with the attached membrane, and only the luminal side subsequently purified by use of detergents. By resolving this luminal membrane fraction by gel electrophoresis and staining with various lectins (see figure legend), the result is as presented in Figure 13.

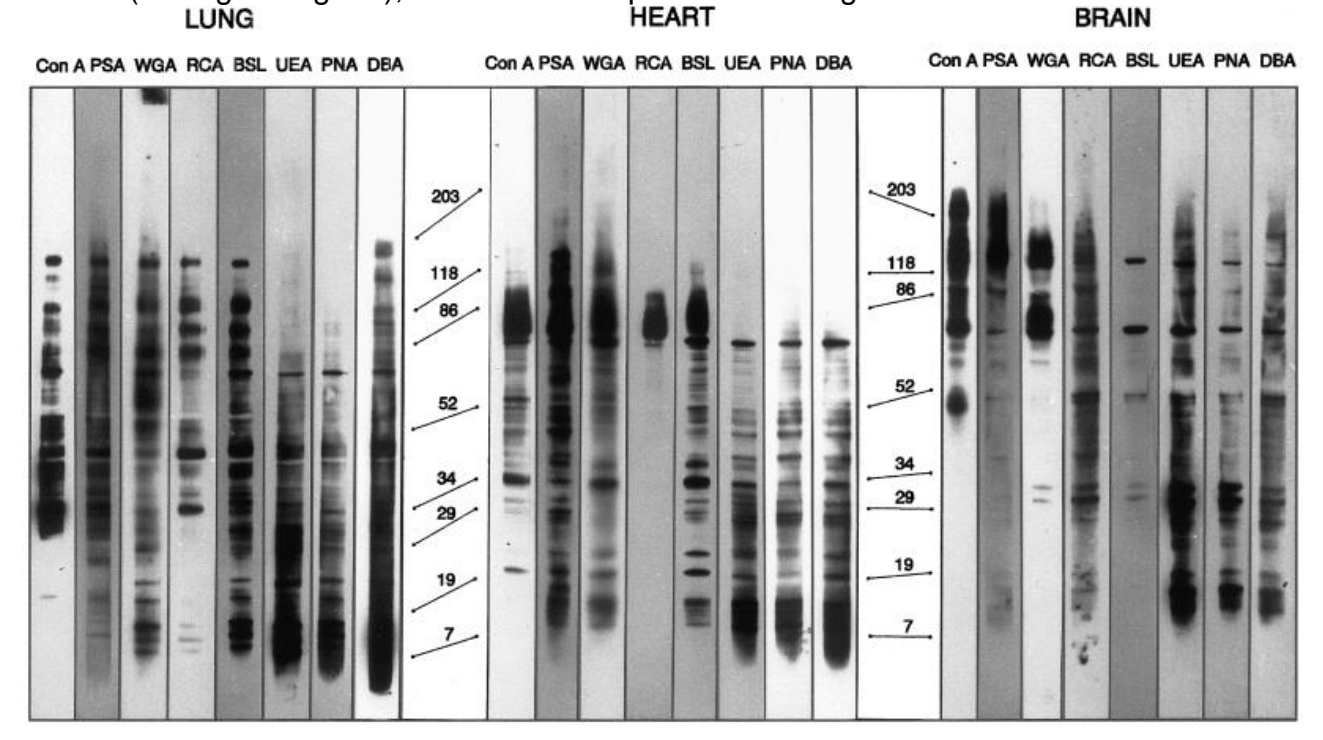


Figure 13. Comparative lectin blotting of the endothelial membranes of lung, heart, and brain microvasculature (P3 fractions). Eighty micrograms of each P3 fraction were loaded on each lane, resolved by SDS-PAGE, transferred to nitrocellulose, and blotted with a panel of biotinylated lectins [each binding the corresponding glycoprotein]: Concanavalin A (ConA) and Pisum Sativum Agglutinin (PSA) (both recognizing α -linked mannose), Wheat Germ Agglutinin (WGA) (specific for N acetyl glucosamine), Ricinus Communis Aglutinin (RCA-I) (Galactose), Bandeirea (Griffonia) Simplicifolia (BSA), Dolichos Biflorus Agglutinin (DBA) (Nacetyl galactosamine), Peanut Agglutinin (PNA) (terminal galactose), and Ulex Europaeus Agglutinin (UEA) (α -linked fucose). (Adapted from Ghitescu and Robert (2002).

Staining with the various lectins (Fig. 13, legend), hereunder WGA that is used in fluorescent microscopy studies mentioned herein, illustrates that there are quite different proteins present in the different vascular beds. These different lectins are available in fluorescent forms, not just WGA. Hence, it would be informative to repeat 2-photon studies with some of these lectins to see how they stain the EC surface in the brain microvasculature. From the gels in Figure 13 are seen a big difference in protein composition, and given mass spectroscopy (MALDI-TOF), it would likely be of interest to revisit and investigate these bands one by one to see if they are all known to be present in the brain EC membranes or whether some should be novel or perhaps surprisingly well known but not for their presence in a purified brain EC GCX fraction.

3. EMERGENCE OF THE FUNCTIONS OF THE GLYCOCALYX AS A DYNAMIC COMPONENT OF BLOOD VESSELS' ENDOTHELIAL CELLS

Most work on the GCX has been done on peripheral vessels and there are still few studies on brain GCX owing to technical difficulties. We will now present some important examples of functions of the GCX that have been discovered since Starling, Vimtrup, Krogh, Hama, Bennett and Luft, and knowledge of which also is applicable to the GCX function in the brain. To the extent data are available, we shall later turn more specifically to brain GCX, with suggestions as to how this more than 100 years of research is now entering a new phase, where it may be possible to understand, prevent and/or even dream about curing diseases affecting functions of the brain.

3.1 The revised Starling Principle: the surprising impact of the subglycocalyx space In medical schools worldwide, we have all been taught the Starling Principle that concerns liquid transudation from and reabsorption by blood vessels. Though this topic may seem off track in terms of giving an account of GCX functionalities, we shall see that to the contrary, actually, the GCX has a surprising big impact on this basic principle which leads to the Revised Starling principle that may, debatably, be of clinical interest in the applied practical fluid treatment of hypovolemic intensive care patients (Woodcock and Woodcock, 2012). This topic has been debated for decades and remains debated and there are still things we do not understand in this context because so many physical, chemical and biological principles and mechanisms are at play simultaneously. We will quickly jump to the connection between the GCX and the Revised Starling principle that started to be published around 1970, although accounts of it dates later back. Yet, it is worthwhile to look at the experiments Starling did to arrive at his principle and an account may be found in section 7.3 (p. 41) of the Supporting Information appendix.

Starling's experiments (Starling, 1896) laid out the ground for research that has been ongoing ever since. The Starling Principle is illustrated in Figure 14 (A1,A2, left side; the legend is on p. 20). We see the balance between fluid filtration and absorption over the arterial and the venous side, respectively. In Figure 14A2, we see this listed in the Starling terms. At the time it was thought that the interstitial pressures (hydraulic and oncotic) were negligible. Consequently, only the P_c (hydrostatic pressure in capillary) and the π_c (oncotic pressure in capillary) would matter, and along the arterial-venous journey, P_c would drop below π_c on the venous side resulting in absorption.

Yet, Starling was unaware of the GCX, could not measure the interstitial pressure, and since microvascular walls really are permeable to proteins (σ =0.9), the osmotic and hydrostatic pressure difference across represent not an equilibrium state but rather a steady state.

Hence, the interstitial hydraulic pressure (P_i) has around 1990 been determined in the human arm to be slightly negative at - 2mmHg and with an osmotic pressure (Π_i) of +15.7 mmHg. This affects greatly the consequence of the liquid flow according to the Starling equation: $J_v/A = Lp((P_c-P_i)-\sigma(\Pi_c-\Pi_i))$ (Fig. 14 A2) because the Π_i is so large. Thus, given this data, there would only be filtration along the vascular bed as illustrated by the black arrows (Figure 14B1; and equation 'Net force classically opposing P_c '), even at the venous side, which is counter to the Starlings conclusions. Eventually this filtrate could be removed through the lymphatic system.

However, the GCX turns out to be causing a real change to the Starling Principle. That is illustrated in Figure 14B1 and 14B2. Hence, the structure of the GCX prevents effectively Albumin from reaching the endothelial surface from where transport of liquid takes place to the interstits. Consequently, there is almost no albumin at the endothelial surface, and therefore the oncotic pressure at the surface is very low and approaching zero. That is illustrated in Figure 14B1. This oncotic pressure is called the 'subglycocalyx oncotic pressure', Π_{SQ} , or just Π_{Q} and has a value close to 0 mmHg. The Revised Starling equation

therefore is $Jv/A = Lp((P_c-P_i)-\sigma(\Pi_c-\Pi_{sg}))$. As illustrated with the red arrows, according to $Jv/A = Lp((P_c-P_i)-\sigma(\Pi_c-\Pi_{sg}))$, we see there only is filtration occurring along the entire vascular bed - thus, no vascular venous reabsorption. In support of filtration, the net lymphatic flow back to the blood stream - stemming from fluid transport over the blood vessels - is estimated to 8 liters/day of which half is estimated to be transported via microlymphatic vessels (reviewed by Levick and Michel (2010)).

However, when we look at it, P_i is slightly negative, so it contributes to filtration, and Π_{sg} is zero, so $\sigma\Pi_c$ is what opposes filtration. Roughly then, when P_c exceeds $\sigma\Pi_c$ there is filtration and when P_c is lower than $\sigma\Pi_c$, e.g. on the venous side, there is absorption; equivalent with what Starling's Principle states, so this does not seem to be right. Yet, surprisingly, this turned out to only be true under transient conditions when there was no time for extravascular forces to change. Hence, under steady state conditions, when Pc was maintained for minutes, no liquid absorption occurred even when P_c was lower than $\sigma\Pi_c$ and contrary to the Starling reabsorption model. This finding has been experimentally verified in various model systems (Levick and Michel, 2010). To explain this, the 'sum of forces'principle applies. Thus, there is obviously a coupling between the oncotic pressure exerted by the extravascular protein concentration (and hence Π_i , measured to +15.7 + 2.8 mmHg in the human arm) and the filtration rate. Hence, under steady state conditions, the fluid that should be absorbed by the vessel lumen when P_c is lower than $\sigma\Pi_c$, remains in the interstits due to the positive Π_i . Indeed, the 'new' interphase established in the subglycocalyx compartment, because of the presence of the GCX, negotiates oncotic pressure with both the vessel lumen and the interstits in terms of its contribution to the direction of fluid transport. The net result is filtration (red arrows, Fig. 14B1; Graphical Abstract).

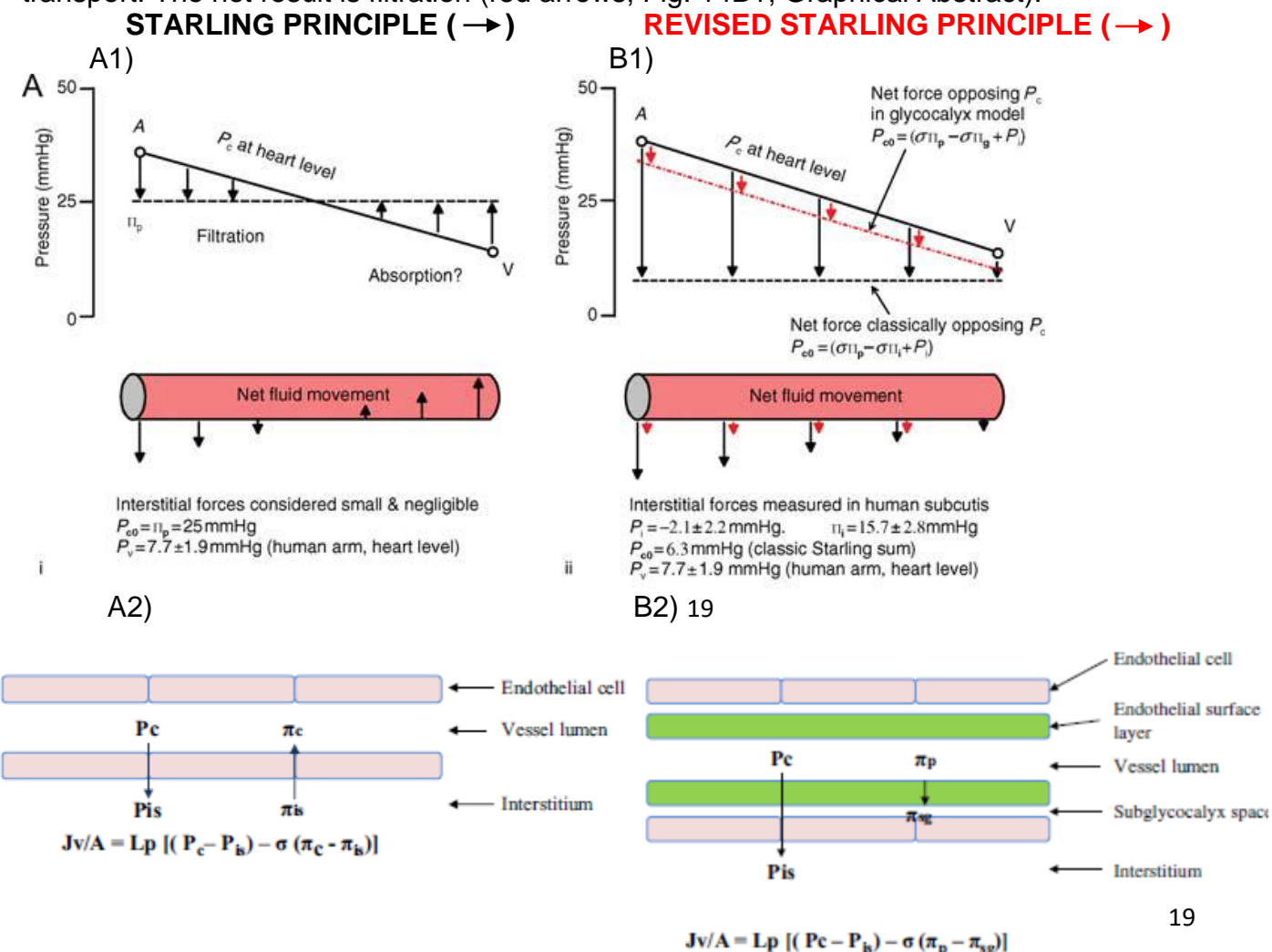


Figure 14 (p. 19). The Starling Principle (A) and the Revised Starling Principle (B). *A1*, Shows the traditional Starling filtration–reabsorption model (A (left) is the arterial side and V (right) is the venous side); interstitial terms are considered negligible; A2, show the corresponding Starling equation. B1, Shows the imbalance when all four classic Starling forces are measured in human skin and subcutis at heart level (A (left) is the arterial side and V (right) is the venous side); the *black arrows* indicate net force imbalance and hence the direction and the magnitude of fluid exchange (only filtration, no absorption); the *dot-dashed red line and arrows* illustrate qualitatively the much smaller net filtration force predicted by the subgglycocalyx–cleft model called the Revised Starling Principle. B2, Shows the corresponding Revised Starling equation, where π sg approaches 0. Terms in equations: J_v/A , volume filtered per unit area; Lp, hydraulic conductance; Pc, capillary hydrostatic pressure; Pis, interstitial hydrostatic pressure. σ, osmotic reflection co-efficient. πc capillary oncotic pressure that is the same as the πp oncotic pressure on plasma-side of endothelial surface layer; πs, interstitial oncotic pressure; πs, oncotic pressure in the subglycocalyx space. (Adapted from (A) Levick and Michel (2010), and (B) Alphonsus and Rodseth (2014)).

Many experimental and theoretical considerations have now established the 'Revised Starling Principle'. The new addition is the addition of the endothelial GCX as an integral part of the blood vessels in the entire body, including in the brain. Hence, the GCX is so dense and has such mechanical properties that the oncotic pressure difference in Starling's equation is not to be taken across the endothelial wall but across the GCX (illustrated in Figure 14B2). The physiological consequence is that during blood flow from the arterial to the venous side, there is only filtration occurring from blood vessels and no reabsorption of fluid, as predicted by Starling. Instead, the filtrated fluid, about 8 liters/day, returns to the blood stream via the lymphatics. Only in the intestines and the kidneys, we have a system where there is filtration on the arterial side and resorption of fluid on the venous side of the vascular bed.

3.2 The glycocalyx influences blood flow and is anywhere in the body an active component of endothelial cells' signaling

Most of the foundational knowledge on the GCX structure, composition and functions comes from studies done on peripheral blood vessels, as mentioned. In terms of function, it has been reported that an intact GCX is associated with good health and that damaged endothelial GCX may play a role in many diseases as for example infectious diseases, diabetes, cancer, and cardiovascular diseases such as atherosclerosis, hypertension and stroke (reviewed e.g. by Francekovic and Gliemann (2023) and Milusev et al. (2022)). As example, we already saw how an erythrocyte passing through capillaries does not make direct contact with the endothelial plasma membrane because of the GCX layer (see Fig. 3, right; Luft (1971)). This has captured interest for decades and is thought to be an essential feature of blood vessels' anticoagulation system, preventing blood clot formation (Milusev et al., 2022).

However, it is no longer necessary to apply advanced microscopic EM methods to observe that erythrocytes and other cells flowing through capillaries are prevented by the GCX from direct interaction with the surface of the EC plasma membrane. For example, and of interest in a medical clinical context, a simple commercial live Sideview Dark Field (SDF) based video imaging system, marketed as the GlycoCheck System (https://glycocheckpro.com/), is now available and used for research. Here, superficial capillaries under the tongue in humans are imaged with a hand-held camera, appearing much like a mouth thermometer, and the output variable is the Perfused Boundary Region (PBR) around the erythrocytes. With this SDF imaging method, it has been determined that the GCX apparently diminishes with age in humans (Figure 15 A). The technical rationale is that a leukocyte cannot penetrate the GCX and therefore compresses it up to 80%, when the vessels are small (5-

8 μm in diameter). Then, erythrocytes, flowing just behind the leukocyte, are observed. Research has namely shown that they tend to flow through the capillary with a slightly wider flow-column width (called the Perfused Boundary Region (PBR)), than if flowing through on their own, i.e. without the leukocyte paving their way by compressing the GCX on the flow path. It is then considered that this change in PBR (flow-column width) is correlated with the GCX thickness (Figure 15 A; (Machin et al., 2018)). E.g. a narrower flow-column width (PBR) is because the GCX is thicker and hence restricts the flow of the erythrocytes more. The determination of the PBR is done by an automated GlycoCheck software, which at pixel level analyzes the green reflected light (540 nm) from the erythrocytes in the superficial capillaries of the tongue in order to define and calculate the PBR.

Erythrocytes passing vessels alone, without leukocytes paving the way, turn out also to have a wider flow path in older versus younger individuals, measured again as change in Perfused Boundary Region (PBR). This is then explained by the older individuals' vessels having GCX that is more penetrable than in young individuals (Figure 15B). The SDF technique has also been tried and works on peripheral cerebral blood vessels in mice that may be reached following craniotomy.

Although these findings and conclusions may appear overly simple, or even farfetched, the experimental approach is simple and fits with experimental observations and theoretical analysis relying on actual intravital microscopy of the vessels in young and old individuals. Therefore, this GlycoCheck System approach may well be of relevance as a read-out in a clinical setting, to test for example a drug's treatment effect on the GCX in a clinical trial. Or perhaps it may one day be used as a basic standard clinical measurement in the overall assessment of a person's health status - the 'body GCX status' - much like the measurement of body temperature.

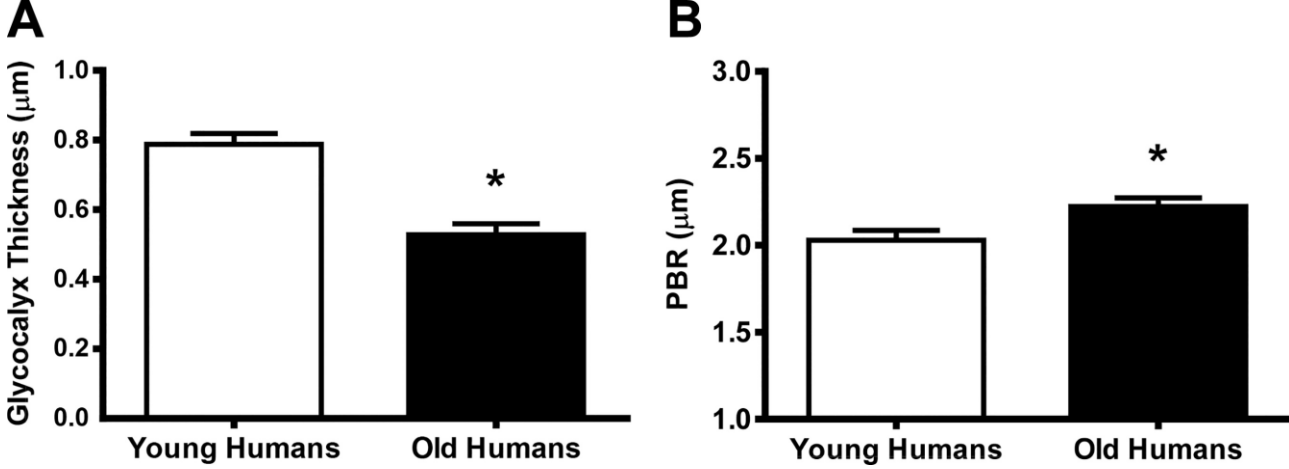


Figure 15. Glycocalyx thickness (A) in sublingual microvessel segments (5–8 μ m) and perfused boundary region (PBR; B) in sublingual microvessel segments (5–25 μ m) of younger and older human participants (n = 30 participants/group). *P = 0.05, significant difference vs. younger participants. All data are means \pm SE. (From (Machin et al., 2018)).

Mechanistically, only few data are available on how the GCX is involved in regulating biological processes. Here also, we must turn to peripheral vessels for well-studied examples.

For example, experiments indicated that fibroblast growth factor (FGF), which is positively charged, is captured by the negatively charged HS in the GCX and oligomerizes (DiGabriele et al., 1998). This oligomerization is required for its cognate FGF receptor (FGFr) to dimerize and its receptor tyrosine kinase signaling activity to be activated in the ECs. Thus, FGF

signal activation requires participation of the GCX. Moreover, it turns out specific HS patterns bind different FGFs (Allen et al., 2001). In later studies, large scale Molecular Dynamics studied were made to model the interaction of HS in GCX and soluble FGF in real time (see Graphical Abstract; Cruz-Chu et al. (2014)); the GCX acts as a 'flypaper' that increases the FGF concentration leading to FGF oligomerization that makes for the activation of the FGFr. We shall not develop further on these studies, as they concern the periphery, but stop and think that similar processes evidently are at work in the brain GCX.

3.3 The GCX can sense shear-stress and convert it to NO signaling and vascular tone A landmark in GCX research is discovery of the GCX's ability to sense shear stress of the flowing blood with subsequent transformation into intracellular signaling and downstream nitric oxide (NO (g)) production (Tarbell and Pahakis, 2006). Metaphorically, the GCX has been compared with 'wind in the trees' during a storm, where the swaying of the tree trunks - representing the stiffer ordered (Arkill et al., 2011) membrane bound proteoglycan foundation of the GCX (See Fig. 11-12) - transmit signals across the endothelium to the intracellular compartment. Soluble components in the blood, the numerous erythrocytes in particular and hence not just the fluid, are a crucial component for the GCX ability to sense sheer-stress. This has been verified through theoretical comparisons applying either the Navier-Stokes equation or the Brinkman equation. The latter makes a better prediction as it includes shear-stress contributions on the GCX from both solid and fluid components in the shear stress calculation, whereas the former only considers the fluid (Foote et al., 2022). Experimentally, it has been demonstrated that a healthy GCX is required - though not absolutely mandatory - for the coupling to NO synthesis in the endothelial cytoplasm by the endothelial NO synthase (eNOS; see Figure 12 and legend (p. 40)). NO can diffuse out of the cell, as it has low molecular weight and is uncharged, NO is notably known for its involvement in lowering blood pressure by relaxing vessels' smooth muscles. It has been hypothesized that people with poor GCX, like for example diabetic patients, have a poorer regulation of their blood pressure which adds to the severity of the disease.

Interestingly, it turned out that shear-stress applied to *in vitro* cultures gives a thicker GCX layer although one could perhaps imagine it would be the opposite. Therefore, current *in vitro* models preferentially incorporate GCX studies in chambers where controlled shear-stress can be induced onto the culture system in e.g. microfluidic lab-on-a-chip devices (see Graphical Abstract). Shear-stress are small forces, measured in dyne/cm², and equaling a few Pa (N/m²), where ambient air pressure in comparison is 1 atmosphere or 10⁵ Pa. At present, it seems that current *in vitro* models lack inclusion of a static blood pressure though it may be of importance.

In the brain, it is also thought that GCX is involved in blood pressure regulation through the shear-stress regulated eNOS. However, to what extent this is the case is unknown and NO blood pressure regulation seems to represent a case that may be of larger importance in the peripheral vessel system than in the brain. Or perhaps the brain has just more ways of regulating vasculature contractility than the peripheral system. Hence, in the brain, the pericytes appears to be crucial in regulating blood flow at the smallest capillary level. Though shear-stress may be a factor, and pericytes can respond to NO (Hall et al., 2014), it seems the pericytes in small capillaries regulate their contractile status rather by diffusible local signals (arachidonic acid, and NO from nNOS) coming directly from and as result of neuronal activity (Hall et al., 2014), and not primarily derived from shear-stress onto the ECs.

Moreover, later studies suggest that local signals include notably K⁺ and Ca²⁺ coming from nearby neuronal activity causing hyperpolarization in these pericytes (Longden et al., 2023).

Through peg-socket junctions (PSJ), the hyperpolarization is transmitted to the local ECs and from there propagated to upstream arterioles, where the hyperpolarization is passed to smooth muscle cells (SMC) through myoendothelial gap junctions. In the SMCs, voltage-sensitive Ca²⁺ channels are then closed, resulting in a lower cytosolic Ca²⁺ concentration, and consequently leading to a vasodilation, as the actin-myosin contractive cycle is interrupted, which ultimately increases the blood flow into those small downstream capillaries that sent the hyperpolarization signal as a result of neuronal activity (Longden et al., 2023). This sophisticated electrical signaling system, to fine-tune blood flow according to local metabolic needs, was recently discovered and is, as reviewed by Longden et al. (2023), found in both the brain and heart vascular systems.

3.4 The glycocalyx is a component of the tripartite blood-brain barrier

The BBB, with its cellular components (Figures 4-8), has for more than 100 years been known as very important for protecting the brain and maintaining homeostasis but what about the GCX?

Mechanistic studies on the functioning of the GCX in brain, like for example the mentioned FGF studies on peripheral vessels, are not yet available. For starters, therefore, just addressing whether the GCX contributes to the BBB is obviously very important. Indeed, one question that arises is whether it can be demonstrated live *in vivo* whether brain ECs have restricted permeability owing to the GCX and whether the GCX thusly contributes to the BBB? This hypothesis appears plausible, in particular given knowledge gained about the subglycocalyx space from formulation of the Revised Starling Principle (section 3.1).

This question has been studied by Kutuzov et al. (2018) using 2-photon microscopy on live mice through a 2-3 mm cranial window (Kucharz et al., 2022a; Kutuzov et al., 2018; Graphical Abstract). Mice were injected with fluorescent dye (representing small molecules) and fluorescently labelled dextran of 40 kDa or 150 kDa (as model for larger molecules) and their distribution at the BBB analyzed (Fig. 16). The BBB was defined by labelling the BBB on its luminal side with injected fluorescently labelled Wheat Germ Agglutinin which binds the GCX (WGA-Alexa; binds HS), and on the abluminal side staining the astrocytes by application of the SR101 stain applied to the brain surface. The study shows convincingly that the GCX is a component of the BBB. It concludes that the BBB consists of three resistors in series going from the vessel's lumen, namely: the GCX, the endothelium and the extravascular compartment (Fig. 16, left panel with legend). The partition coefficients (α_g) into the GCX, defined as the ratio between fluorescence in the center of the vessel and the center for the GCX, of the tested molecules were found to be: $\alpha_{g,NaF}=0.95$, $\alpha_{g,AF}=0.94$, $\alpha_{g,Dex40}$ =0.48, $\alpha_{g,Dex150}$ =0.31, $\alpha_{g,Dex150_Hase}$ =0.75 (Fig. 16, right panel). It is seen that α_{g} drops when the molecular weight increases, as expected. Likewise, upon treatment with hyaluronidase, to remove the GCX, the $\alpha_{g,Dex150_Hase}$ for Dex150 approaches the α_g for the fluorescent dyes, showing that the GCX is a molecular weight filter. Not surprisingly it was found that the fluorescent intensity (I(t)) inside the vessel is proportional with the flux (J(t), [cm/s]) of fluorescence away from the vessel - through the BBB - and this flux is likewise proportional to the concentration in the GCX (Figure 16, right panel with legend). Hence, transport across the endothelium could be described by its permeability (P. [cm/s]). As shown in table 1, there is a clear correlation between molecular weight and permeability (P). When the endothelium was subject to Mannitol, that disrupts the cell-cell tight-junction interactions due to osmotic cellular shrinking of the endothelium, there was as expected a measurable increase in P of the tested Dex150 (Figure 16, table 1); values for P after GCX hyaluronidase treatment are not reported but are also expected to increase.

From this study, we see the GCX is part of the BBB, consisting of 1) the GCX, 2) the ECs connected by tight junctions and 3) the extravascular compartment (Figure 16A, resistors).

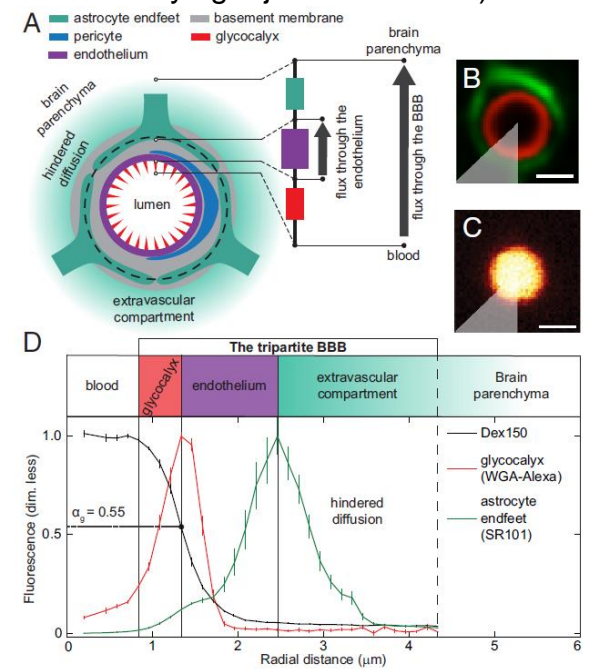


Figure 16. Components of the tripartite BBB. Glycocalyx and astrocyte endfeet were labeled and used as landmarks to locate the components of the tripartite BBB on recorded images. (A) Simplified diagram showing the main components of the BBB. The BBB was partitioned into three compartments - GCX (red), endothelium (purple), and extravascular compartment (green) - based on their functional transport properties (GCX partition coefficient (α), permeability (P), and diffusion coefficients (D*)) revealed by the data. The transport properties of these three compartments are analogous to three Ohmic resistors connected in series (schematic on the right side in A; see the Discussion in the paper for more explanation). Thus, for a given concentration difference across the BBB, the GCX and the extravascular compartment reduce the drop in concentration across the endothelium, and hence reduce the flux through it, in a manner that depends on the type of molecules in question.(B) GCX (red) and astrocyte endfeet (green) were labeled with WGA-Alexa and SR101, respectively. (C) Distribution of Dex150 fluorescence in the vessel lumen (the intensity is normalized by its maximum value). (D) Radial intensity profiles were obtained by selecting a sector (gray area, in B and C) and averaging the pixel values located at the same distances (x axis) from the center of the vessel lumen (SI Appendix, Fig. S1 in the paper). The maxima of WGA-Alexa and SR101 fluorescence intensities defined the inner and outer boundaries, respectively, of the endothelium. The partition coefficient, α_g , is the ratio between the fluorescence intensities of the dye at the peak of the WGA-Alexa distribution (red in B: the GCX laver) and in the plasma (C). Error bars were estimated, as described in SI Appendix, Statistics. (Scale bar, 2 µm.)

Table 1. Diffusion coefficients (D*), endothelial permeabilities (P), and reaction constants (k_r) for NaF, AF, Dex40, and Dex150

Molecule	D^* , 10^{-8} cm ² /s	P , 10^{-7} cm/s	k_r , $10^{-2} \mathrm{s}^{-1}$
NaF [†]	1.30 ± 0.16 (8)	3.91 ± 0.41 (8)	6.3 ± 1.4 (8)
AF [†]	1.25 ± 0.09 (8)	3.95 ± 0.18 (8)	0.8 ± 0.6 (8)
Dex40 [†]	0.55 ± 0.07 (8)	1.40 ± 0.15 (8)	2.6 ± 0.5 (8)
Dex150 [†]	0.19 ± 0.06 (8)	0.51 ± 0.14 (8)	1.7 ± 0.5 (8)
Dex150‡	0.25 ± 0.07 (6)	0.62 ± 0.17 (6)	2.3 ± 0.6 (6)
Dex150 ^{†,§}	0.18 ± 0.06 (8)	0.38 ± 0.09 (8)	3.1 ± 0.8 (8)
Dex150 ^{†,} ¶	0.27 ± 0.05 (6)	1.24 ± 0.20 (6)	1.5 ± 0.7 (6)

Data represent the mean \pm SEM of **n** independent measurements.

D*: is the diffusion coefficient of the dye in the extravascular compartment.

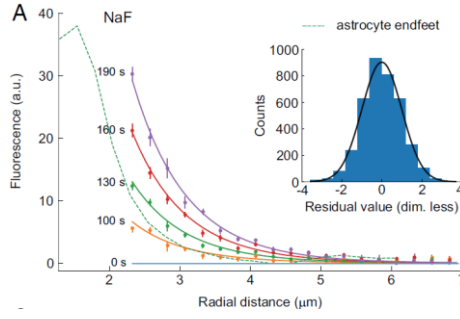
P: is the *permeability* of the vascular endothelium.

kr: photobleaching reaction constant.

Diameter: the luminal vessel diameter.

The flux J(t) across the endothel was proport. to the

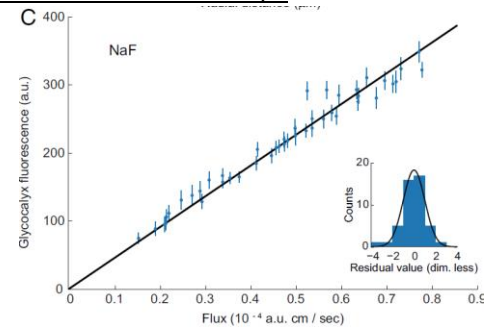
measured extravascular fluorescent intensity I(t,r) away from the vessel shown in (NaF shown; time is in seconds (s)).Moreover, analysis showed that fluorescent flux (J(t)) away from the vessel simply was



proportional to fluorescence in the GCX.

Then, plotting GCX fluorescent intensity I(t) [y-axis] against fluorescent flux J(t) [cm/s], obtained by fitting the data in (A), the **permeability** (P) [cm/s] can be approximated to: $J(t) = \alpha_g P K I(t)$, α_g and K are constants, and P can then be estimated from J(t)/I(t), which is the inverse of the slope of the

straight line, shown in C 400 C. ((Kutuzov et al., 2018), materials and methods, Fig. 3 and SI).



[†]Diameter \approx 3–5 μm

[‡]Diameter > 10 μm.

[§]Intracarotid injection of saline (control).

[¶]Intracarotid injection of mannitol.

However, this study (Fig. 16) is just using markers of the BBB. What If we now try to look at the GCX's contribution to the BBB in the context of the biologically active BBB, which has both transport and signaling of biological active molecules as well as subsequent effects on the brain parenchyma? Then we have an even more complex situation. A degraded BBB may also affect transport of waste material *away from* the brain, and there the GCX also is of importance given it is part of the BBB, as we shall look at in the context of neurodegenerative diseases.

Now, figure 17 depicts the types of biological transport mechanisms involved in BBB crossing. Note that the GCX is omitted from Fig. 17, as it is still not standard to include it as part of the BBB.

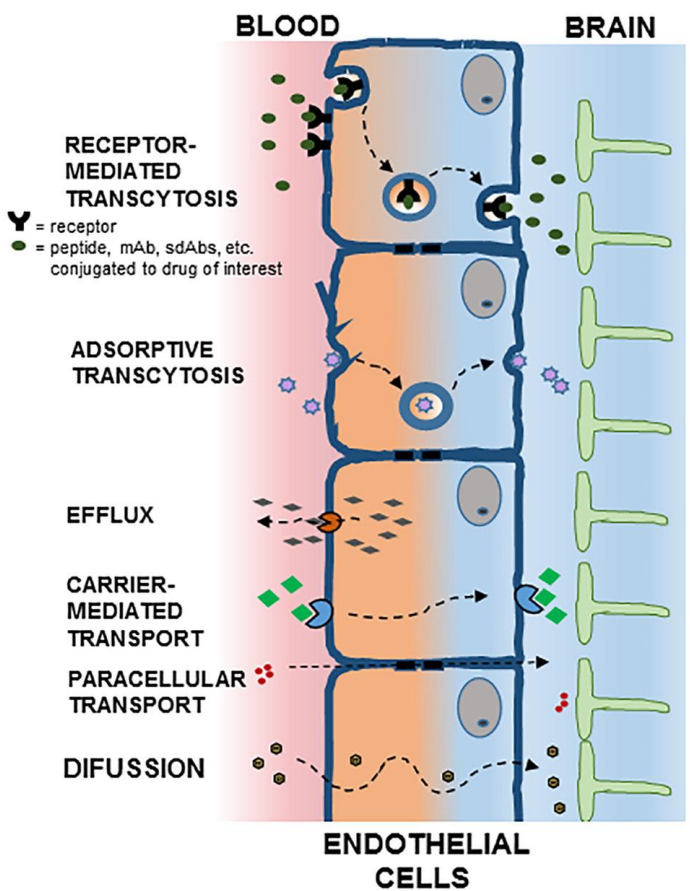


Figure 17. Potential mechanisms for crossing the blood brain barrier (BBB). Polarized endothelial cells, bound by tight junctions, form a seal that controls free movement or molecules from blood to brain. In brain capillaries, endothelial cells are in intimate association with astrocytes (green) demarcating the outer boundary of the BBB of the NVU (see Fig. 7-8). Potential mechanisms for crossing the BBB are indicated: (A) Receptor Mediated Transcytosis; (B) Adsorptive Transcytosis (AT); (C) Efflux; (D) Carrier-Mediated Transport; (E) Paracellular Transport; (F) Diffusion. [Note: the GCX layer is omitted from this figure]. (Adapted from Pulgar (2018).

Let's try to look at transport across the BBB, focusing on the GCX involvement, to the extent data are available. For example, *Adsorptive Transcytosis* (*AT*, Fig. 17; it is non-specific transport) is notably known to increase in correlation with poor health and neurological conditions. Increased AT is used as a marker for decreased BBB function. Do these

observations perhaps have to do with poor GCX? One study could demonstrate that enzymatic removal of the GCX increased AT across the BBB and that knock-down of caveolin-1 prevented this increase (Zhu et al., 2022; caveolin-1 is described in Fig. 12, p. 40). Another study also showed similar effect of increased AT correlating with decreasing GCX, which was achieved through impaired S1P signaling in *Apomr*/- knockout mice (S1P is carried by Apom, its *absence* lowers the free S1P plasma concentration; S1Pr activation protects the GCX; see Fig. 12 legend bottom, p. 41). Interestingly, only the GCX in arterioles was affected by the impaired S1P signaling and not in venules or capillaries. However, although restoring the S1P signaling did restore lower levels of AT, it did not restore the GCX (Kucharz et al., 2022b).

Thus, the two studies both showed increase in AT upon GCX removal but could not demonstrate a correlation between the restoration of the GCX and lowering AT. Hence, it did not appear that presence of the GCX was a prerequisite *per se* for low AT.

The studies are representative for brain endothelial GCX studies, namely that they remain at an early stage, where there still is a lack of convincing data showing the impact of the GCX on important processes involving the BBB, apart from cases like sepsis with GCX removal resulting in edema. Zhu et al. (2022)) uses e.g. LPS to induce a sepsis-like state. These two studies were done in mice that together with rats are the most used to model the human BBB. However, can these findings really be extrapolated to humans? Not only biological differences but also size and life span differences may be of importance when BBB comparisons are made between rodents and humans.

3.5 The glycocalyx shields the endothelium and receptors and expose them when needed

As described by Luft (1965), the fragile GCX escaped *in vitro* studies for a long time it collapses easily when manipulated. To see the GCX *in vivo* required new techniques such as intra vital microscopy, 2-photon and, earlier, confocal imaging. Doing experiments in brain *in vivo* is additionally challenging. Since the first images, GCX has been hypothesized to provides steric hindrance and negative charge repulsion, and thereby shield the EC surface from unlimited interaction with immune cells, salt and molecules racing by in the blood stream of even the smallest of capillaries. Yet, only the last decade has evidence for these ideas been provided from *in vivo* studies. Most of the hypotheses for the functions of the GCX in brain are relying on GCX studies done in other parts of the body. However, there are differences in GCX composition, as already illustrated by the biochemical analysis of purified luminal EC membranes from heart, lung and brain shown in Figure 13. What these differences between brain and periferal GCX mean functionally still need further analysis.

This is not to say that there are no similarities between GCX in different parts of the body. Indeed, we shall now look at an important example of GCX function in peripheral vessels that turned out later to show strong similarities to seminal findings in brain capillaries in the context of neurodegenerative diseases. In this study (Schmidt et al., 2012) show that injection of lipo-polysaccharide (LPS) into mice blood vessels causes rapid degradation of the GCX in lung endothelium but not in the cremaster muscle arterioles. This elegant study illustrates for the first time *in vivo* how the GCX sterically hinders cellular binding to the EC membrane. In Figure 18 (a) is seen the model system. FITC-labelled 150 kDa dextran is injected in mice and the width of the lung microvessel available to perfusion can then be measured by comparing the DIC and the FITC image (i.e. the DIC image includes the width of the GCX whereas the FITC channel excludes the width of the GCX).

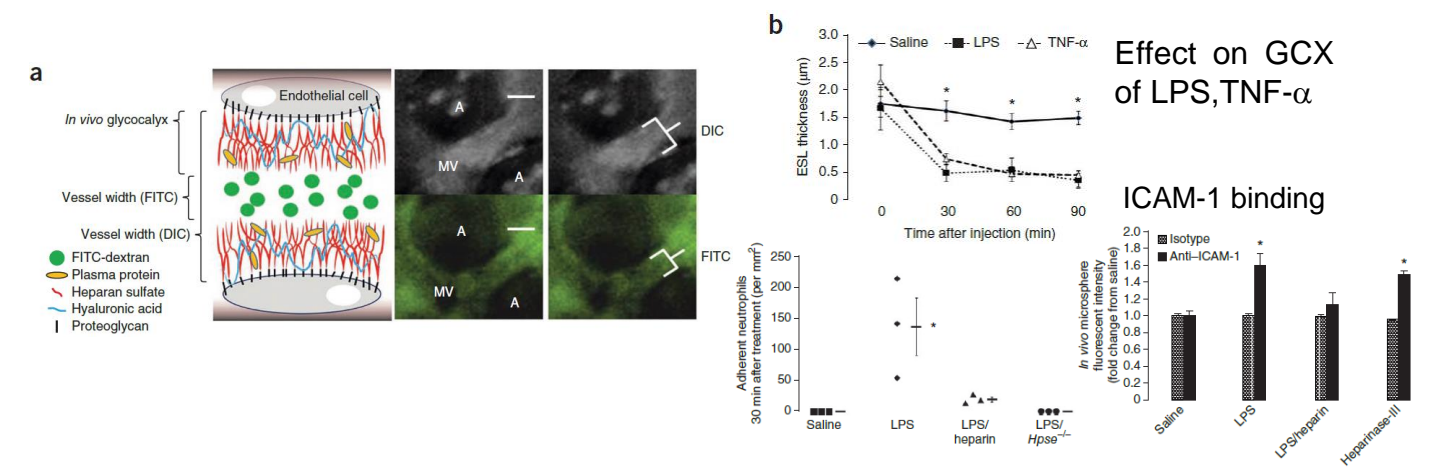


Figure 18. Mouse lung microvessels *in vivo*, showing GCX thickness, GCX binding of neutrophils and ICAM-1 antibody staining. (a) Microvessel perfused with 150 kDa dextran, and plotted in (b); GCX (ESL=External SurfaceLayer) thickness is calculated from (a) as *DIC* minus *FITC* thickness (*A* is alveola, *MV* is MicroVessel); b,top GCX (ESL) thickness following saline (control), LPS or TNF-a treatment. (b,bottom); *left* shows number fluorescently labelled neutrophils bound; LPS/heparin: LPS and heparin simultaneously, LPS/Hpse-/-: LPS injected in a homozygotic Heparanse knockout mouse; *right* shows normalized intensity (to saline) of ICAM-1 antibody coated microspheres, binding exposed ICAM-1/CD54 on the ECs, following shown treatments (Heparanase is more specific and cleaves HS into fragments whereas heparinase-III extensively cleaves HS). (Adapted from Schmidt et al. (2012)).

Figure 18(b, top) shows that following LPS treatment the GCX thickness drops significantly by more than 1 μ m. LPS is a surface coating present on many bacteria, and the innate immune system is programmed to respond to such through Toll receptor activation (Abbas et al., 2024). That activation can be reproduced by injection of TNF- α which is a cytokine released early in sepsis and upon LPS exposure (Fig. 18b, top). After injection of fluorescently labelled neutrophils, they measure binding to the GCX. Yet, only following LPS treatment is binding observed (Fig. 18b, bottom). With LPS plus heparin, there is no effect, as heparin is an inhibitor of activation of the LPS pathway. Neither is there in a heparanase knockout mouse effect of LPS, as the LPS treatment requires release of heparanase from the endothelium to degrade the GCX (Fig. 18b, bottom left).

As the experiments demonstrate, removal of the GCX increases the binding of the innate immunoresponse's neutrophile cells to the EC. Hence, ICAM-1 is one of the adhesion molecules involved in binding the neutrophiles to the ECs. Exposure of ICAM-1, demonstrated by anti-ICAM-1 antibody binding, correlates with neutrophile binding (Fig. 18b, bottom right). In sum, the experiments provide evidence for the hypothesis that the GCX covers receptors on the EC and uncovers them when the GCX is removed. Figure 19 presents a cartoon of their results.

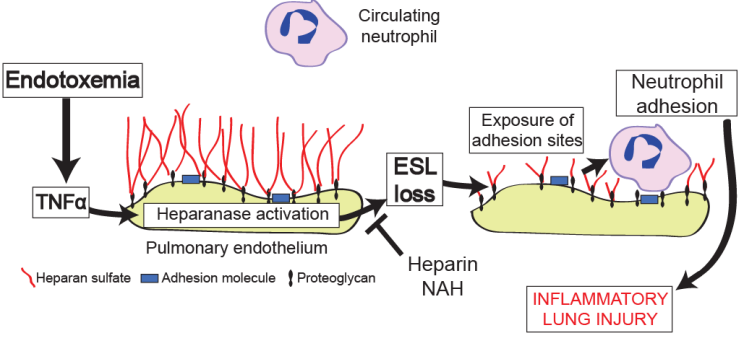


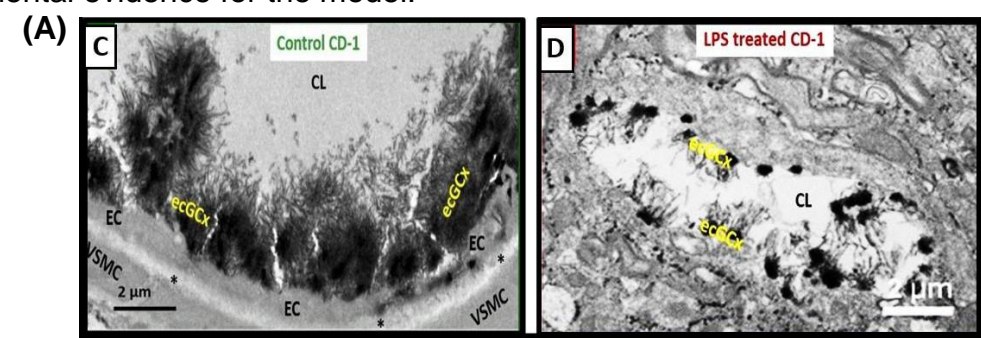
Figure 19 (p. 27). Proposed model for the heparanase-GCX signaling during LPS exposure/sepsis described by Schmidt et al. (2012). *Left*, in a healthy animal, neutrophils are excluded from interaction with the endothelial surface by the GCX. *Right*, upon exposure to LPS, or to the cytokine TNF-a, heparanase is activated, its expression increases and it is released extracellularly, where heparan sulfate (HS) in the GCX is degraded, which leads to decreased GCX thickness. HS degradation, while only partial, is sufficient to lead to increased exposure of neutrophil adhesion molecules (like ICAM-1) on the cell surface. Inhibition of heparanase by heparin (NAH, nonanticoagulant heparin) is sufficient to block GCX degradation. (Adapted from supplementary information in Schmidt et al. (2012)).

While the Schmidt et al. (2012) experiments may seem straightforward to carry out, they have only been possible the last decade, as knock-out mice, intra vital microscopy, microsphere and coating technologies are required. The current assumption is that very similar principles are governing the brain endothelial GCX, as we shall see in the next section. Moreover, they estimate that the lung GCX *in vivo* has a thickness of as much as 1,67 μ m, which is twice of what had been measured in systemic circulation in the cremaster muscle (Smith et al., 2003). They hypothesize that this may be to protect the lung from inadvertent influx of immune cells. This hypothesis echoes much the thinking concerning the GCX's function and contribution to the BBB in the brain.

4. EXPERIMENTAL EVIDENCE FOR A ROLE OF THE GLYCOCALYX AS PART OF THE BLOOD-BRAIN BARRIER *IN VIVO*

Now, along the lines of (Schmidt et al., 2012), experiments focused on the brain GCX in CD-1 mice following LPS treatments *in vivo*, have recently been carried out. They support the notion that the GCX is an important component of the BBB (Erickson et al., 2023; Hayden, 2023). The LPS exposure experiments are analyzed by EM using the LAN staining of Ando et al. (2018) and provide very interesting images. Following the LPS treatment, the GCX was removed (Figure 20A). In the postcapillary venules an enlarged perivascular space (ePVS) was obtained following the LPS treatment (Figure 20B; although this is the only image they obtained). Nevertheless, it supports that GCX removal provokes BBB breaching and subsequent migration of cells into the interstitial space. They propose a model where GCX degradation results in BBB disruption, followed by edema and diapedesis of immune cells into the PVS (step 1) and further into the neuropil (step 2), where inflammation and neurodegeneration may ensue (Figure 20C, Graphical Abstract). We will later return to this model in the context of Alzheimer's disease.

Unfortunately, there are only few images available in the study. However, the model has been proposed for decades, and images are worth bringing in this context because there, as mentioned already, still only is little data available looking directly at the GCX in brain and its function in health and disease and because these images are the first to provide some experimental evidence for the model.



(B)

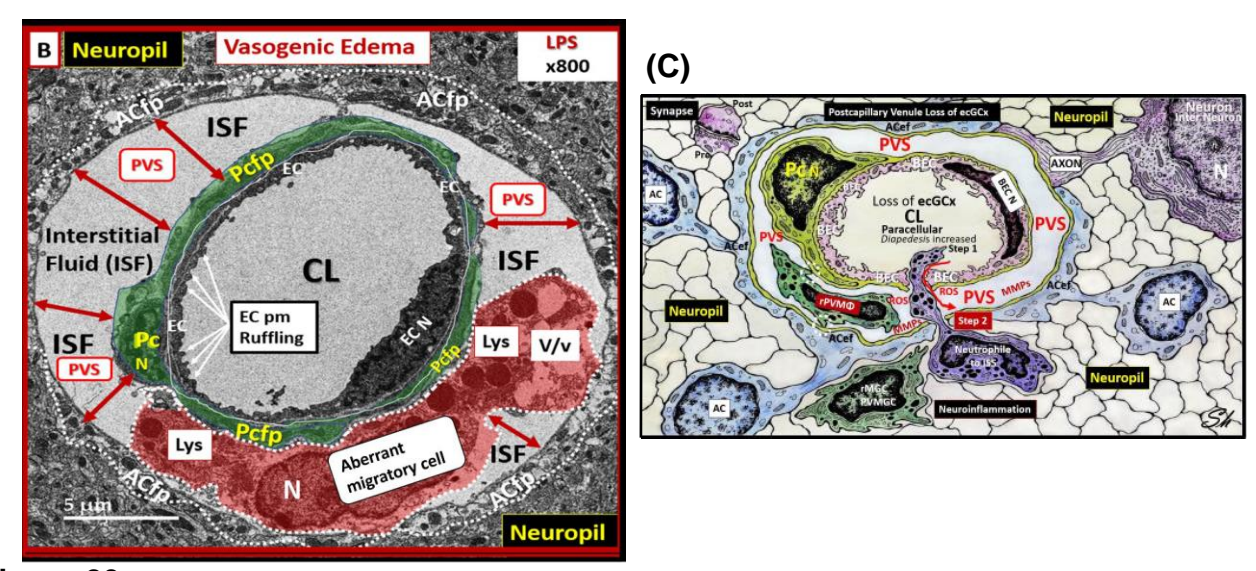


Figure 20. Loss or attenuation of the endothelial GCX (ecGCx; (A, p. 28)) LPS treatment results in ecGCx removal with subsequent NeuroVascular (NVU) Blood-Brain Barrier (BBB) disruption with increased permeability to fluids, cytokines and chemokines, cells and notably inflammatory leukocytes. (B), In postcapillary venules, eGCX loss results in: step 1, BBB disruption by leukocytes and their entering into the PeriVascular Space (PVS) together with fluid; step 2: breaching of the outer basement lamina of the PVS due to inflammatory oxidative stress and MMP damage of the AC and an ensuing enlargement of the perivascular space (ePVS). (C) Shows a model of (B), including step 1 and step 2; Note the red arrow denoting that after ecGCX degradation, there will in step 1 be increased fluid entering the perivascular space (PVS) as well as transmigration of proinflammatory leukocytes into the PVS, and also note the breech in step 2 of the PVS itself, as depicted by the purple-colored neutrophile via the outermost basal laminae of the astrocyte endfeet (ACef), and migration into the interstitial space of the neuronal parachyma resulting in neuroinflammation. Importantly, note the red arrow denoting (step 1) the loss of fluid and solutes from the capillary lumen to the PVS with ensuing enlargement. Additionally, tight and adherens junctions will become aberrant making the paracellular breech possible. Importantly, note the complete loss of the brain endothelial cell (BEC) GCX in the depicted NVU capillary (B). AC = astrocyte; ACfp = astrocyte foot process; ACef = astrocyte endfeet; BEC = brain endothelial cell; CL = capillary lumen; EC = brain endothelial cells; ISF= interstitial fluid; Lys = lysosome; ISS = interstitial space; MMPs = matrix metalloproteinases; $N = nucleus; Pc = pericyte; Pc N = pericyte nucleus; rPVM \Phi = resident, reactive perivascular macrophage; ROS = reactive$ oxygen species; TJ/AJ = tight and adherens junctions; V = vacuole; v = vesicles. (Figures and legend adapted from (Erickson et al., 2023; Hayden, 2023)).

The role of the GCX in the BBB was also focus in other experiments using a rat model simulating cardiac arrest (CA, 8 minutes) followed by CPR resucitation. Following CA/CPR, (Zhu et al., 2018) could demonstrate by EM an impaired GCX in capillaries in the hippocampus as well as increased expression of inflammatory markers (i.e. ICAM-1, VCAM-1 and MembraneMetalloProteinases (MMPs)), loss of neurons and microglial and astrocyte activation. Interestingly, impairment of the GCX could be mitigated by hydrocortisone treatment which also improved survival and lowered the expression of a number of genes, most likely due to the downregulation of cytokine production and gene expression. When they treated with injection of hyaluronidase (HAse) the effects were more severe than with CA/CPR alone and there could also be observed brain edema. These experiments fit the paradigm that the GCX is an important part of the BBB. The results are consistent with theoretical considerations from other studies on mechanisms of edema development following GCX removal, notably increased paracellular transport owing to TJ/AJ exposure and damage, which likely is both dose and injection site dependent. Indeed, another study uses HAse to lower brain edema in a mouse model following contusion brain injury (Washington et al., 2020). The rationale is that removal of negatively charged molecules from a surface lowers the Gibbs-Donnan effect (negatively charge surfaces will attract water and positive ions) and thereby mitigate edema formation by reducing the fixed charge density that water can adhere to (Washington et al., 2020). These researchers injected 0.03 Unit HAse/g mouse *into the ventricles* (ICV injection), whereas (Zhu et al., 2018) used 0.01 Unit HAse/g rat injected *intravenously*. Importantly, by injection into the ventricle, HAse has access to the opposite side of the BBB (CSF compartment) compared to HAse injected intravenously by (Zhu et al., 2018). Washington et al. (2020) show by MR that ICV injection indeed lowers edema and check, by MRI, that there does not seem to be any change in BBB integrity, indicating an unaffected GCX following ICV injection of HAse. Washington et al. (2020) does not quote the Zhu et al. (2018) study and only uses MRI techniques to support their claims.

Taken together these two studies are interesting, as they also render support to the importance of the concept that drug delivery to the right compartment may be crucial for the wanted outcome. However, it appears following the Zhu et al. (2018) results that usage of HA to treat edema by ICV injection potentially is a hazardous procedure that likely could not be applied to treat brain edema in human patients. Moreover, it has been raised as a possibility that the brain vasculature is more sensitive to enzymatic ways of removing the GCX, like with HAse, so the severity of the HAse treatment in Zhu et al. (2018) to some extent may be an artefact (O'Hare et al., 2024). This is important to keep in mind when thinking about designing experiments to test for the effects of the absence of the GCX. Hence, it may not be advisable to use HAse. If it were possible to make inducible transgenic mice targeting specifically the brain GCX that would seem like a good model, but at present such mice are not available.

Contributions to corroborate that the GCX is an important part of the BBB have been gathered from other both *in vivo* (Yang et al., 2021; Zhu et al., 2022) and *in vitro* (DeOre et al., 2022) studies.

5. POSSIBLE INVOLVEMENT OF THE GLYCOCALYX IN NEURODEGENERATIVE DISEASE ETIOLOGY

In this section, we will look at the possible involvement of the GCX in neurodegenerative diseases and notably Alzheimer's disease. Often descriptions of neurodegenerative diseases, hereunder Alzheimer's, are centered on the symptomatic outcome, namely the observable behavioral changes over extended time intervals, often decades, as a result of, in part, observable neurodegeneration. However, it is becoming more and more clear that neurodegeneration in Alzheimer's only occurs late in disease progression. Description of Alzheimer's has traditionally focused on three observable pathological hallmarks in the brain parenchyma, namely extracellular amyloid $(A\beta_{1-42})$ deposition, hyperphosphorylation and tangles in neurons, and overactivation of microglial (phagocytic cells in the brain). Lately, PET scanning of the posterior parietal cortex is also used diagnostically, as decreased glucose uptake there is seen in Alzheimer's. Indeed, it is gathering momentum that changes in the brain's vascular system, and other processes, likely occur much earlier in Alzheimer's disease than mentioned classic hallmarks. In this context, the microvascular BBB with associated GCX, is receiving interest. However, part of this interest is fueled by the fact that there are still no remedies, and much less cures, available to stop neurodegenerative diseases like Alzheimer's - therefore there is a need to look elsewhere.

If we look at known risk factors for acquiring sporadic Alzheimer's (LOAD), ageing is the biggest risk factor. It therefore seems obvious to investigate whether there is a change in

GCX as a function of age. Interestingly, (Machin et al., 2018) report that in systemic vessels, GCX in aged mice and humans is 30-50 % thinner in younger individuals as measured by IVM (see Figure 15A). The brand new Shi et al. (2025) study supports this notion (Shi et al. (2025; Fig. 1b,c) and Graphical Abstract). These observations can be coupled with the finding that cerebral blood flow (CBF) is decreased by ~25 % early in Alzheimer's disease development, both in Alzheimer mouse models and in humans; moreover, this decrease appears to correlate with an increased tendency of the neutrophil leukocytic cells to stall and plug capillaries in mouse brains (Cruz-Hernandez et al., 2019).

Here, we briefly recall the in section 3.5 described experiments that also concerned leukocytes' interaction with ECs' GCX following LPS treatment in mouse lung arterioles (Schmidt et al., 2012) and brain capillaries (Erickson et al., 2023).

Importantly, in Cruz-Hernandez et al. (2019), reversing the decreased CBF in the Alzheimer mouse models - by using an antibody against the Ly6G neutrophil surface marker - also resulted in a rapidly and over hours improved performance in both spatial and working memory tasks, and return to normal after a month. However, the anti-Ly6G antibody treatment also resulted in complete neutrophil depletion that will have immunosuppressive effects that, however, were not addressed in the study.

In support of these findings, another group has in mice tried to manipulate the GCX in brain and by IVM and 2-photon microscopy observed that there is increased neutrophil stalling when the GCX is impaired, either enzymatically or by induction of vascular dementia by surgically induced blood flow constriction through the common carotid artery (Yoon et al., 2022). These data suggest that enzymatically decreasing GCX increases neutrophil stalling and that this also is the case in the vascular dementia mouse. These experiments ran over two months. During that time, there was no observable change in the control neutrophil stalling, as compared to the vascular dementia model mouse. Hence, we do not have a direct read-out where we can see that aging promotes increased neutrophil stalling, and that this correlates to decrease in GCX, as the (Machin et al., 2018; Shi et al., 2025) studies suggest. However, this may be because these experiments only run over two months - the (Shi et al., 2025) studies ran over 18 months - which may not be long enough for age to show an effect. Indeed, this may be an important point where mouse models differ from humans where longer time spans are possible, rendering one-to-one comparisons difficult between human and mice. As mentioned, the (Shi et al., 2025) study provides some evidence against this.

Returning to the Cruz-Hernandez et al. (2019) experiments, they showed increased neutrophil stalling in the standard Alzheimer's mouse models APP/PS1 and 5xFAD. In an interesting model simulation (Figure 20), where they compare the observed stalling in mice and extrapolates that to the human cortex by using knowledge of the anatomy and blood flow in the human brain. For example, at stalled blood flow in 20 % of capillaries (Fig. 20c, x=0.20) there would only be 55 % cerebral blood flood (y=0.55) compared to normal (no stalled capillaries). The model-simulation indicates that the stalling observed in mice would cause the same effect on CBF in humans, and hence stalling could possibly have a similar contribution to the development of Alzheimer's. Given the mentioned (Yoon et al., 2022) data, it is tempting to speculate that these effects may be the result of, in part, a decrease in GCX which Cruz-Hernandez et al. (2019), however, did not also investigate. Hence, there is room for repeating these experiments and look at the GCX.

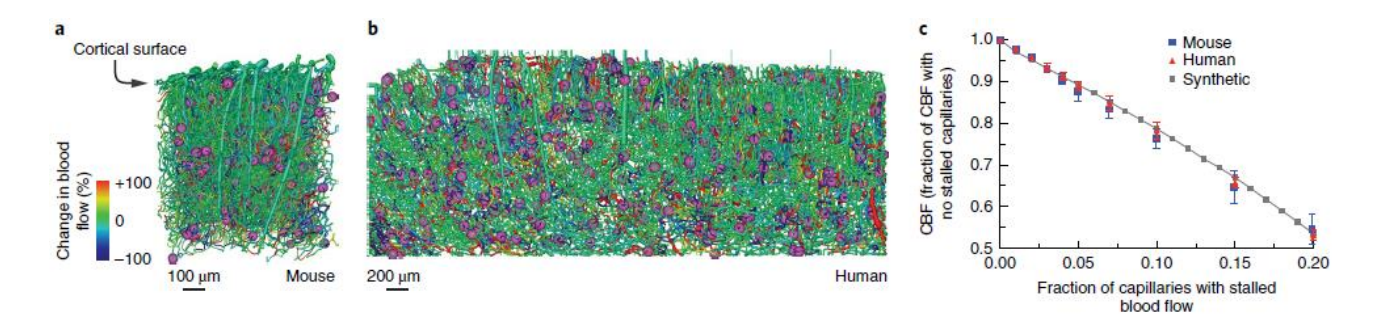


Figure 20. Neutrophil stalling in modelled mouse (a) and modelled human cortex (b) correlates, when compared with controls without stalling, with decreased cerebral blood flow (*CBF*, (c), y-axis) and is a linear function of the fraction of capillaries with stalled blood flow (x-axis). (adapted from Cruz-Hernandez et al. (2019)).

5.1 Glycocalyx' possible role in human Alzheimers' progression and treatment

Alzheimer's is currently the neurodegenerative disease affecting the most people in the world, the number is only expected to rise in the coming decades, and there is still no cure or effective remedy to relieve or slow down its progression. The GCX has possibly for this reason become a hot topic in this context, as the prevalent amyloid deposit and tau tangling neurocentric view hypothesis of Alzheimer's has not given results, as mentioned. For example, the latest attempts at using antibody therapies to remove amyloid plaques, named Aduhelm approved in 2021 by FDA and its successor Donanemab, have once again proven a dead end and been taken off the markets. Aduhelm does remove plaques but this does not necessarily correlate with improvement in symptoms, and as all immunotherapies, it can have severe side-effects, like brain edema and bleeding, is quite costly and labor intensive to administer. Pharmaceutical companies are very reluctant to step into Alzheimer's because nobody, so far, has managed to provide a treatment with a sufficiently positive effect for the patients. The neurocentric view may possibly be a wrong paradigm to apply when wanting to treat Alzheimer's disease. When neuronal damage has occurred, as in late Alzheimer's, there has been an irreparable irreversible process.

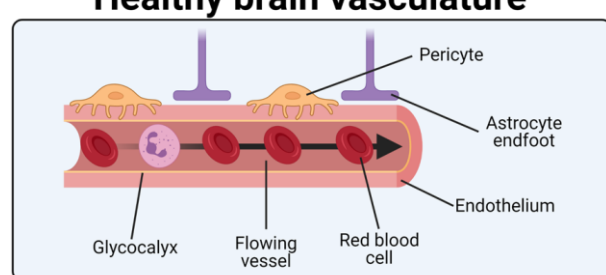
Focus of novel pharmaceutical products should probably be on preventing Alzheimer's, and halting progression, as that probably is what can be expected from drugs. Moreover, a potential treatment should ideally be easy to administer and control because so many people are at risk. In fact, considering aging is the biggest risk factor, all humans are at risk of acquiring Alzheimer's at late life. Ideally, a remedy like a vitamin pill, such as for example C-vitamin that has stopped incidents of scurvy, should be developed. It looks like the GCX may have such properties, if it were possible to stimulate ECs to maintain an adequate layer of GCX and thereby maintain an intact BBB. Interestingly, Shi et al. (2025) transfect mice with adenovirus expressing novel glycoproteins that are densely O-glycosylated and known as so-called mucin-domain type glycoproteins (see Graphical Abstract top) which repairs the GCX in aged mice, which however is not readily an option, if the purpose is to treat human patients. Nevertheless, research in recent decades confirms that Alzheimer's is detectable by vascular defects occurring long before neurodegenerative symptoms are observed.

A study in humans submits that increased neutrophil adhesion is correlated with a decrease in GCX and increase in Alzheimer progression (Smyth et al., 2022), similar to the (Cruz-Hernandez et al., 2019; Yoon et al., 2022) studies. Moreover, using an immuno-microarray from human AD brain, and staining against lectin (GCX), they show there is significantly less GCX than in the control. Interestingly, using an RNAseq atlas of the AD brain vasculature (made by Yang et al. (2022)), they find decreased expression of *FUT11* in

ECs, where FUT11p is an enzyme involved in GCX production. This finding is corroborated by the Shi et al. (2025; Fig. 2m) study, which describes that synthesis of the mucin-domain glycoproteins, they find downregulated in aged mice, involves amongst other downregulation of *FUT11* transcription.

The main tenant is that the attachment to ECs and access of the neutrophils through the BBB likely in part is due to a damaged GCX. Inside the parenchyma, the neutrophils then cause damage to the neurons, presumably to a large extent due to their very reactive myeloperoxidase (MPO) content. Their proposed model based on these human data is shown in Figure 21, which mirrors the model based on mouse studies shown in Figure 20.

Healthy brain vasculature



Alzheimer's disease vasculature

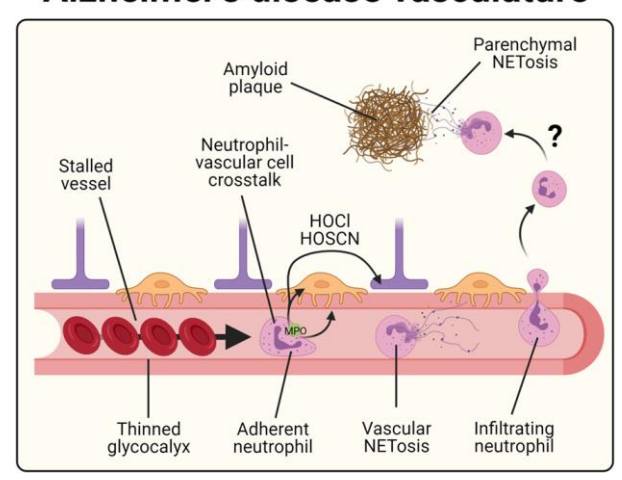


Figure 21. Effects of neutrophil-vascular interactions in AD. *Left*, in healthy brains, neutrophils flow freely through vessels with limited interactions with ECs enabling adequate perfusion. Right, during Alzheimer's disease, reductions in the GCX may enhance the non-productive attachment of neutrophils to endothelial cells. These attached neutrophils can cause stalling of vessels, undergo NETosis (Neutrophile Extracellular Trap cell death pathway triggering ET formation and surrounding tissue toxicity), and may lead to oxidative stress and BBB breakdown. In AD, reducing neutrophil-vascular interactions may be beneficial to improve vascular function. (Adapted from Smyth et al. (2022)).

The Shi et al. (2025) study adds novel very interesting discoveries to the GCX puzzle through the discovery and functional analysis of the two B3gnt3p and C1galt1p mucin-type O-glycan biosynthesis pathway enzymes. Initially, they just observe that the GCX gets thinner in aged mice compared with young mice (18 months difference). That is the starting observation. By using a bulk brain EC RNA-sequencing library and comparing young and aged mice, they then analyzed that there were changes in expression of glycosylation related genes with age (Figure 22).

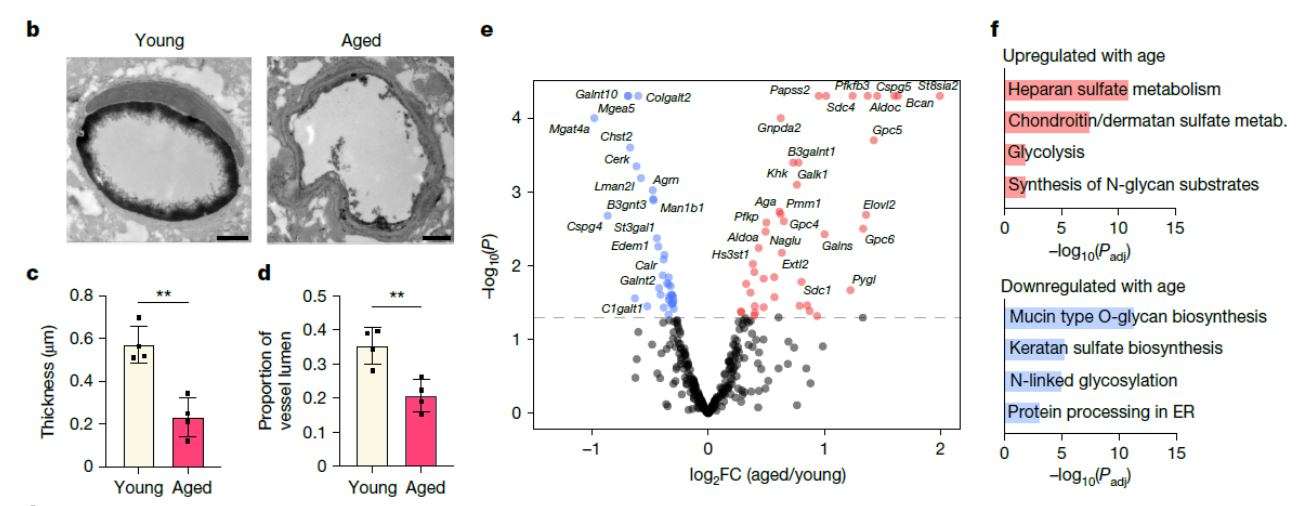


Figure 22. The brain endothelial glycocalyx is highly dysregulated during ageing, discovery of B3gnt3p and C1galt1p. **b**, TEM of cortical capillaries with lanthanum nitrate staining from young (3-month-old) and aged (21-month-old) mice. Scale bars, 1 μ m. **c**, Quantification of luminal endothelial glycocalyx thickness of young (3-month-old) and aged (21-month-old) mice (n = 4 mice per group; two-sided t-test; mean \pm s.e.m.). **d**, Quantification of luminal endothelial glycocalyx area of young (3-month-old) and aged (21-month-old) mice (n = 4 mice per group; two-sided t-test; mean \pm s.e.m.) [see also Graphical Abstract, bottom]. **e**, Volcano plot of differentially expressed glycosylation-related genes in brain endothelial cells from young (3-month-old) and aged (19-month-old) mice (genes upregulated with age in red and genes downregulated with age in blue). Original bulk RNA-seq data are from Yousef et al. (ref. 12 in that paper). **f**, Top glycosylation-related pathways that are upregulated and downregulated with age in brain endothelial cells. ER, endoplasmic reticulum; metab., metabolism. (Adapted from Shi et al. (2025)).

They could then show this correlated with significantly decreased expression of mucin-domain glycoproteins by staining with fluorescently labelled StcE(E447D) [a mutant of an enzyme that degrades mucin glycoproteins]. Moreover, they could go on and downregulate these two enzymes in *young* mice using knock-down techniques by adenovirus infection *in vivo* and show that the GCX became thin, as in aged mice. In these mice the BBB was found to be more leaky. If they injected the active StcE enzyme and waited for two days, they could remove the StcE(E447D) staining, and widespread BBB dysfunction and unexpected cerebral haemorrhaging with noticeable red blood cell leakage in the meninges and ventricles was observed. This is somewhat similar to the results reported by Zhu et al. (2022) following Heparanase treatment. Furthermore, they could express these two enzymes in old mice by adenovirus infection and restore the GCX thickness as if they were young mice.

The study is the first of its kind in that they are able to show *in vivo* that removal of a glycosylation related enzyme decreases the GCX coating (thickness and/or area covered), *AND* that this is reversible by (over) expressing these enzymes in old mice. Moreover, they also report that these enzymes are found downregulated in human AD brains.

If all of this was not enough, they were also able to show that old mice that expressed the C1galt1p enzyme behaved comparable to young mice in a behavioral Y maze test after 12 weeks Shi et al. (2025).

They write in their study, they during their datamining found many additional brain EC glycosylation pathways that were dysregulated in ageing and neurodegenerative diseases. Hence, there are options for performing further exciting experiments perhaps more focused on the earlier mentioned Syndecan, Glypican, HS, and HA parts of the GCX.

It sounds reasonable that an unbroken GCX both can block neutrophil stalling and neutrophil access to the brain parenchyma, which otherwise could contribute to induce inflammation, cellular and neuronal damage and impose stress on the NVU altogether. However, there is still not firm evidence to put forward a model that holds such a mechanism as primary cause leading to Alzheimer's. We can think that having an unbroken GCX in the brain may be best, but it likely is just adding weight to negative risk factors for Alzheimer's, rather than bringing us further to a potential treatment to prevent the disease. Many are the suggestions for dietary supplements that can be taken to improve GCX, hereunder i.v. treatment with thiosulfate, but it is very doubtful that it will have an impact as big as mentioned effect of C-vitamin on scurvy.

The strong correlation between the incidence of Alzheimer's and age is a clear indication that just as death then also Alzheimer's, to some extent, is an inevitable consequence of being alive, and finding a cure may therefore be unlikely. Though such viewpoint may seem pessimistic, and unlikely to gather research funding, it may be a good attitude to avoid spending too many resources on new dead ends. Indeed, there may not be a miracle cure. As an example, recently the noble gas Xenon (Xe) has made noise in the Alzheimer's field. Experiments reveal that in mouse models, inhalation of 30 % Xe over 40 minutes - making it possible to use on humans - is enough to activate microglial cells to be more active at removing amyloid plaques (Brandao et al., 2025). Apparently, Xe passes the BBB and activates gene transcription. Although interesting, there may be unforeseen side effects if applied on humans. For example, Xe's gene specificity did not evolve with the human transcriptome and it may block NMDA receptors.

While the number of cases continues to rise steadily, it will be interesting to follow research on Alzheimer's in the coming decades. It seems that the GCX is playing a central role as part of the BBB, but we still lack actual experimental facts in humans to support this notion and how it perhaps affects Alzheimer's development over time.

If we try to go with the hypothesis that brain endothelial GCX, as part of the BBB, is implicated in the etiology of Alzheimer's disease, in order to advance and find potential treatments, it seems pivotal to: **a**) combine *in vitro* and *in vivo* approaches. The brain does not make for a good model system to screen potential treatments; they are better found by applying BBB *in vitro* systems that keep getting more *in vivo*-like with the inclusion of endothelial cells, astrocytes, microglial, neurons and pericytes as well as flow that simulates the pulsating *in vivo* blood flow shear-stress (see Graphical Abstract, right). **b**) In *in vitro* systems, apply novel gene tools like CRISPR/Cas9 to modify cell lines specifically targeting the GCX to screen for changes in BBB properties and screen for potential new drugs effects. New inspiration for gene candidates to test may be obtained from the Shi et al. (2025) study.

With such systems it may be tested whether any agents (apart from recombinant adenovirus) can be found that e.g. result in overexpression of the mucin-domain glycoproteins in order to counter the GCX loss with age. So far, no prescription medications targeting specifically preservation of the GCX have been made available. Whether the promise of the GCX as a therapeutic target for patient treatment will result in the production of GCX specific drugs remains at best likely but uncertain and difficult to predict.

c) *In vivo* it would be worthwhile to take the already existing mouse models for Alzheimer's (ie. APP/PS1, 5xFAD) and check them thoroughly for eventual changes in GCX as a function of time. Indeed, from the Shi et al. (2025) study, we saw they by LAN EM could see a significant change in GCX after 18 months using the standard wild-type laboratory C57BL/6J mouse. **d**) It would be very useful to develop *conditional* EC specific GCX knockouts of GCX core components (i.e. conditional knockouts of Syndecan, Glypican, Mucin-domain

glycoproteins or enzymes involved in glycosylation), as removal of the GCX with enzymes, such as HA, is difficult to control and with side-effects. Such knockout mice could then be crossed with already existing Alzheimer model mice, to see whether introduction of defects in the endothelial GCX results in more severe symptoms, has a synergistic effect, or perhaps have no effects. **e**) Further development of improved and novel imaging methods, examining the BBB in humans, by e.g. QUTE-CE MRI, in the context of longitudinal human epidemiological cohort studies starting at early age. Such would be informative as to the correlation between BBB function and development of Alzheimer's and could be analyzed for the contribution of the GCX.

As a closing remark we have herein looked at the EC GCX and, as is clear, there is still room for much advancement in knowledge. It is early days in this field. Here it should be said that the ECs are producing the GCX, which then gets somewhat modified upon interaction with the bloodstream. Hence, the ECs are the source of the GCX. Full understanding of the ECs' genetic programming and regulation must constitute an integral part on the road towards further understanding of the endothelial cell GCX during health and disease, whether that be in brain or systemic vessels.

6. REFERENCES

Review articles

- Abbas, A.K., Lichtman, A.H., and Pillai, S. (2024). Basic Immunology: functions and disorders of the immune system, 7 edn (Canada: Elsevier). 345 pp.
- Alberts, B., Hopkin, K., Johnson, D., Morgan, D., Raff, M., Roberts, K., and Walter, P. (2019). Essential Cell Biology, 5 edn (W.W. Norton and Company). 734 pp.
- Alphonsus, C.S., and Rodseth, R.N. (2014). The endothelial glycocalyx: a review of the vascular barrier. Anaesthesia *69*, 777-784.
- Becker, B.F., Chappell, D., and Jacob, M. (2010). Endothelial glycocalyx and coronary vascular permeability: the fringe benefit. Basic Res Cardiol *105*, 687-701.
- Dancy, C., Heintzelman, K.E., and Katt, M.E. (2024). The Glycocalyx: The Importance of Sugar Coating the Blood-Brain Barrier. Int J Mol Sci *25*. 8404.
- Daniele, S.G., Trummer, G., Hossmann, K.A., Vrselja, Z., Benk, C., Gobeske, K.T., Damjanovic, D., Andrijevic, D., Pooth, J.S., Dellal, D., *et al.* (2021). Brain vulnerability and viability after ischaemia. Nat Rev Neurosci *22*, 553-572.
- Deli, M.A., Porkolab, G., Kincses, A., Meszaros, M., Szecsko, A., Kocsis, A.E., Vigh, J.P., Valkai, S., Veszelka, S., Walter, F.R., *et al.* (2024). Lab-on-a-chip models of the blood-brain barrier: evolution, problems, perspectives. Lab Chip *24*, 1030-1063.
- Foote, C.A., Soares, R.N., Ramirez-Perez, F.I., Ghiarone, T., Aroor, A., Manrique-Acevedo, C., Padilla, J., and Martinez-Lemus, L. (2022). Endothelial Glycocalyx. Compr Physiol *12*, 3781-3811.
- Francekovic, P., and Gliemann, L. (2023). Endothelial Glycocalyx Preservation-Impact of Nutrition and Lifestyle. Nutrients *15*, 2573.
- Galea, I. (2021). The blood-brain barrier in systemic infection and inflammation. Cell Mol Immunol *18*, 2489-2501.
- Ghitescu, L., and Robert, M. (2002). Diversity in unity: the biochemical composition of the endothelial cell surface varies between the vascular beds. Microsc Res Tech *57*, 381-389.
- Hajal, C., Le Roi, B., Kamm, R.D., and Maoz, B.M. (2021). Biology and Models of the Blood-Brain Barrier. Annu Rev Biomed Eng *23*, 359-384.
- Hayden, M.R. (2023). The Brain Endothelial Cell Glycocalyx Plays a Crucial Role in the Development of Enlarged Perivascular Spaces in Obesity, Metabolic Syndrome, and Type 2 Diabetes Mellitus. Life (Basel) 13, 1955.

- Krogh, A. (1929). The anatomy and physiology of capillaries, Revised and enlarged edition edn (Yale University Press). 422 pp.
- Kucharz, K., Kutuzov, N., Zhukov, O., Mathiesen Janiurek, M., and Lauritzen, M. (2022a). Shedding Light on the Blood-Brain Barrier Transport with Two-Photon Microscopy In Vivo. Pharm Res *39*, 1457-1468.
- Levick, J.R., and Michel, C.C. (2010). Microvascular fluid exchange and the revised Starling principle. Cardiovasc Res 87, 198-210.
- Longden, T.A., Zhao, G., Hariharan, A., and Lederer, W.J. (2023). Pericytes and the Control of Blood Flow in Brain and Heart. Annu Rev Physiol *85*, 137-164. Milusev, A., Rieben, R., and Sorvillo, N. (2022). The Endothelial Glycocalyx: A Possible Therapeutic Target in Cardiovascular Disorders. Front Cardiovasc Med *9*, 897087.
- O'Hare, N., Millican, K., and Ebong, E.E. (2024). Unraveling neurovascular mysteries: the role of endothelial glycocalyx dysfunction in Alzheimer's disease pathogenesis. Front Physiol *15*, 1394725.
- Parton, R.G., and del Pozo, M.A. (2013). Caveolae as plasma membrane sensors, protectors and organizers. Nat Rev Mol Cell Biol *14*, 98-112.
- Pulgar, V.M. (2018). Transcytosis to Cross the Blood Brain Barrier, New Advancements and Challenges. Front Neurosci 12, 1019.
- Tarbell, J.M., and Pahakis, M.Y. (2006). Mechanotransduction and the glycocalyx. J Intern Med *259*, 339-350. Terstappen, G.C., Meyer, A.H., Bell, R.D., and Zhang, W. (2021). Strategies for delivering therapeutics across the blood-brain barrier. Nat Rev Drug Discov *20*, 362-383.
- Udan, R.S., Culver, J.C., and Dickinson, M.E. (2013). Understanding vascular development. Wiley Interdiscip Rev Dev Biol *2*, 327-346.
- Woodcock, T.E., and Woodcock, T.M. (2012). Revised Starling equation and the glycocalyx model of transvascular fluid exchange: an improved paradigm for prescribing intravenous fluid therapy. Br J Anaesth 108, 384-394.
- Yang, R., Chen, M., Zheng, J., Li, X., and Zhang, X. (2021). The Role of Heparin and Glycocalyx in Blood-Brain Barrier Dysfunction. Front Immunol *12*, 754141.
- Zeng, Y., Zhang, X.F., Fu, B.M., and Tarbell, J.M. (2018). The Role of Endothelial Surface Glycocalyx in Mechanosensing and Transduction. In Molecular, Cellular, and Tissue Engineering of the Vascular System, B.M. Fu, and N.T. Wright, eds. (Springer), pp. 1-27.

Research articles

- Allen, B.L., Filla, M.S., and Rapraeger, A.C. (2001). Role of heparan sulfate as a tissue-specific regulator of FGF-4 and FGF receptor recognition. J Cell Biol *155*, 845-858.
- Ando, Y., Okada, H., Takemura, G., Suzuki, K., Takada, C., Tomita, H., Zaikokuji, R., Hotta, Y., Miyazaki, N., Yano, H., et al. (2018). Brain-Specific Ultrastructure of Capillary Endothelial Glycocalyx and Its Possible Contribution for Blood Brain Barrier. Sci Rep 8, 17523.
- Arkill, K.P., Knupp, C., Michel, C.C., Neal, C.R., Qvortrup, K., Rostgaard, J., and Squire, J.M. (2011). Similar endothelial glycocalyx structures in microvessels from a range of mammalian tissues: evidence for a common filtering mechanism? Biophys J 101, 1046-1056.
- Ballinger, M.L., Nigro, J., Frontanilla, K.V., Dart, A.M., and Little, P.J. (2004). Regulation of glycosaminoglycan structure and atherogenesis. Cell Mol Life Sci *61*, 1296-1306.
- Bennett, H.S. (1963). Morphological-aspects-of-extracellular-polysaccharides. J Hiistochem Cytochem 11(1), 14-23.
- Brandao, W., Jain, N., Yin, Z., Kleemann, K.L., Carpenter, M., Bao, X., Serrano, J.R., Tycksen, E., Durao, A., Barry, J.L., et al. (2025). Inhaled xenon modulates microglia and ameliorates disease in mouse models of amyloidosis and tauopathy. Sci Transl Med 17, eadk3690.
- Cruz-Chu, E.R., Malafeev, A., Pajarskas, T., Pivkin, I.V., and Koumoutsakos, P. (2014). Structure and response to flow of the glycocalyx layer. Biophys J *106*, 232-243.

- Cruz-Hernandez, J.C., Bracko, O., Kersbergen, C.J., Muse, V., Haft-Javaherian, M., Berg, M., Park, L., Vinarcsik, L.K., Ivasyk, I., Rivera, D.A., et al. (2019). Neutrophil adhesion in brain capillaries reduces cortical blood flow and impairs memory function in Alzheimer's disease mouse models. Nat Neurosci 22, 413-420.
- DeOre, B.J., Partyka, P.P., Fan, F., and Galie, P.A. (2022). CD44 mediates shear stress mechanotransduction in an in vitro blood-brain barrier model through small GTPases RhoA and Rac1. FASEB J *36*, e22278.
- DiGabriele, A.D., Lax, I., Chen, D.I., Svahn, C.M., Jaye, M., Schlessinger, J., and Hendrickson, W.A. (1998). Structure of a heparin-linked biologically active dimer of fibroblast growth factor. Nature *393*, 812-817.
- Erickson, M.A., Shulyatnikova, T., Banks, W.A., and Hayden, M.R. (2023). Ultrastructural Remodeling of the Blood-Brain Barrier and Neurovascular Unit by Lipopolysaccharide-Induced Neuroinflammation. Int J Mol Sci *24*, 1640.
- Haeren, R.H.L., Rijkers, K., Schijns, O., Dings, J., Hoogland, G., van Zandvoort, M., Vink, H., and van Overbeeke, J.J. (2018). In vivo assessment of the human cerebral microcirculation and its glycocalyx: A technical report. J Neurosci Methods *303*, 114-125.
- Hall, C.N., Reynell, C., Gesslein, B., Hamilton, N.B., Mishra, A., Sutherland, B.A., O'Farrell, F.M., Buchan, A.M., Lauritzen, M., and Attwell, D. (2014). Capillary pericytes regulate cerebral blood flow in health and disease. Nature *508*, 55-60.
- Hama, K. (1960). The Fine Structure of Some Blood Vessels of the Earthworm, Eisenia foetida. J Biophys Biochem 7, 717-724 (7plates).
- Kucharz, K., Mathiesen Janiurek, M., Christoffersen, C., and Lauritzen, M. (2022b). Two-photon microscopy in vivo reveals brain vessel type-specific loss of glycocalyx caused by apoM/S1P signaling impairment. bioRxiv preprint doi: https://doiorg/101101/20220411487803, 18 p.
- Kutuzov, N., Flyvbjerg, H., and Lauritzen, M. (2018). Contributions of the glycocalyx, endothelium, and extravascular compartment to the blood-brain barrier. Proc Natl Acad Sci U S A *115*, E9429-E9438.
- Leaston, J., Ferris, C.F., Kulkarni, P., Chandramohan, D., van de Ven, A.L., Qiao, J., Timms, L., Sepulcre, J., El Fakhri, G., Ma, C., et al. (2021). Neurovascular imaging with QUTE-CE MRI in APOE4 rats reveals early vascular abnormalities. PLoS One 16, e0256749.
- Luft, J.H. (1965). Fine structure of capillaries: the endocapillary layer. In American Association of Anatomists Seventy-Eighth Annual Session University of Miami School of Medicine, April 20, 21, 22, 23 (The Anatomical Record, V151(pp. 315-502)), p. 380.
- Luft, J.H. (1971). Ruthenium red and violet. II. Fine structural localization in animal tissues. Anat Rec *171*, 369-415.
- Machin, D.R., Bloom, S.I., Campbell, R.A., Phuong, T.T.T., Gates, P.E., Lesniewski, L.A., Rondina, M.T., and Donato, A.J. (2018). Advanced age results in a diminished endothelial glycocalyx. Am J Physiol Heart Circ Physiol *315*, H531-H539.
- Megens, R.T., Reitsma, S., Schiffers, P.H., Hilgers, R.H., De Mey, J.G., Slaaf, D.W., oude Egbrink, M.G., and van Zandvoort, M.A. (2007). Two-photon microscopy of vital murine elastic and muscular arteries. Combined structural and functional imaging with subcellular resolution. J Vasc Res *44*, 87-98.
- Reily, C., Stewart, T.J., Renfrow, M.B., and Novak, J. (2019). Glycosylation in health and disease. Nat Rev Nephrol 15, 346-366.
- Schmidt, E.P., Yang, Y., Janssen, W.J., Gandjeva, A., Perez, M.J., Barthel, L., Zemans, R.L., Bowman, J.C., Koyanagi, D.E., Yunt, Z.X., et al. (2012). The pulmonary endothelial glycocalyx regulates neutrophil adhesion and lung injury during experimental sepsis. Nat Med 18, 1217-1223.
- Shi, S.M., Suh, R.J., Shon, D.J., Garcia, F.J., Buff, J.K., Atkins, M., Li, L., Lu, N., Sun, B., Luo, J., et al. (2025). Glycocalyx dysregulation impairs blood-brain barrier in ageing and disease. Nature (Epub ahead of print). https://doi.org/10.1038/s41586-025-08589-9.
- Smith, M.L., Long, D.S., Damiano, E.R., and Ley, K. (2003). Near-Wall μ -PIV Reveals a Hydrodynamically Relevant Endothelial Surface Layer in Venules In Vivo. Biophys J 85, 637-645.
- Smyth, L.C.D., Murray, H.C., Hill, M., van Leeuwen, E., Highet, B., Magon, N.J., Osanlouy, M., Mathiesen, S.N.,

- Mockett, B., Singh-Bains, M.K., et al. (2022). Neutrophil-vascular interactions drive myeloperoxidase accumulation in the brain in Alzheimer's disease. Acta Neuropathol Commun 10, 38.
- Starling, E.H. (1896). On the absorption of fluids from the connective tissue spaces. J Physiol 19, 312-326.
- van Zandvoort, M., Engels, W., Douma, K., Beckers, L., Oude Egbrink, M., Daemen, M., and Slaaf, D.W. (2004). Two-photon microscopy for imaging of the (atherosclerotic) vascular wall: a proof of concept study. J Vasc Res *41*, 54-63.
- Vimptrup, B. (1922). Beiträge zur Anatomie der Capillaren. I . Über contractile Elemente in der Gefäßwand der Blutcapillaren. Zeit f Anat u Entwickelungsges 65, 150-182 (7 plates).
- Washington, P.M., Lee, C., Dwyer, M.K.R., Konofagou, E.E., Kernie, S.G., and Morrison, B., 3rd (2020). Hyaluronidase reduced edema after experimental traumatic brain injury. J Cereb Blood Flow Metab 40, 2026-2037.
- Yang, A.C., Vest, R.T., Kern, F., Lee, D.P., Agam, M., Maat, C.A., Losada, P.M., Chen, M.B., Schaum, N., Khoury, N., et al. (2022). A human brain vascular atlas reveals diverse mediators of Alzheimer's risk. Nature 603, 885-892.
- Yoon, J.H., Lee, E.S., and Jeong, Y. (2017). In vivo Imaging of the Cerebral Endothelial Glycocalyx in Mice. J Vasc Res *54*, 59-67.
- Yoon, J.H., Shin, P., Joo, J., Kim, G.S., Oh, W.Y., and Jeong, Y. (2022). Increased capillary stalling is associated with endothelial glycocalyx loss in subcortical vascular dementia. J Cereb Blood Flow Metab *42*, 1383-1397.
- Zeng, Y., and Tarbell, J.M. (2014). The adaptive remodeling of endothelial glycocalyx in response to fluid shear stress. PLoS One *9*, e86249.
- Zhu, J., Li, X., Yin, J., Hu, Y., Gu, Y., and Pan, S. (2018). Glycocalyx degradation leads to blood-brain barrier dysfunction and brain edema after asphyxia cardiac arrest in rats. J Cereb Blood Flow Metab *38*, 1979-1992.
- Zhu, J., Li, Z., Ji, Z., Wu, Y., He, Y., Liu, K., Chang, Y., Peng, Y., Lin, Z., Wang, S., et al. (2022). Glycocalyx is critical for blood-brain barrier integrity by suppressing caveolin1-dependent endothelial transcytosis following ischemic stroke. Brain Pathol *32*, e13006.

7. SUPPORTING INFORMATION appendix

7.1 BIBLIOGRAPHICAL ASPECTS OF RESEARCH ON THE BRAIN GLYCOCALYX

We must stop and notice that we herein have presented both molecular, cellular and systemic effects of the GCX that, however, for the most part concern or is evidenced by research from other parts of the body than the brain. Research on the GCX in brain and its involvement in the BBB is namely still in an early phase. This is even more so when it comes to a possible involvement in the etiology of neurodegenerative diseases like Alzheimer's.

To illustrate this, looking at the Pubmed database, and the search phrase 'brain endothelial glycocalyx', there were only seven reviews between 1989 (first review) and 2015, and there have been big gaps; i.e. from 1990 to 1999 there were zero reviews and likewise from 2008 to 2013. In comparison, from 2016 to 2025 there has so far been 36 reviews with an accelerating pace, i.e. from 2020-2025 so far 31 reviews. While this could seem like a field with full speed forward, unfortunately it turns out that real research papers on the 'brain endothelial glycocalyx' only amount to 55 papers from 2020 to 2025, and hence that reviews in this area constitute 36% of the total of only 86 2020-2025 published papers, according to a Pubmed search. If we look at the previous 30 years, from 1989 to 2020, there were just 12 reviews and 73 actual research papers. Thus, from 1989-2019 reviews in this area constituted just 14% of the published material, according to a Pubmed search. Thus, the past 5 five years, the review to research article ratio is up almost 3-fold as compared to the

previous 30 years. For reference, from 1962-2025 there were 2283 entries for 'endothelial glycocalyx' (1962 first reference) of which 544, 24%, were reviews, according to a Pubmed search; 2020-2025 represent 1057 of these papers whereof 278, 26%, were reviews.

That brain GCX is particular, may be seen by comparing with e.g. the 'glutamate transporter' field, where out of 2051 papers published 2020-2025 only 183, or 9 %, were reviews. Even in a field like 'Alzheimer's disease' - that has the attention of the public eye - there were 76,173 papers from 2020-2025 whereof 17,022, or 22 %, were reviews, according to a Pubmed search. (Pubmed: https://pubmed.ncbi.nlm.nih.gov/).

Although there is a tendency, in most fields, that more reviews are published today than in the past, because there are more researchers, more consumers of research and it has become much easier to publish something, it seems in particular skewed in the case of the 'brain endothelial GCX' field. There may be an argument for publishing many reviews to draw attention to this field and discuss hypothesis and to attract more research and/or funding. However, all these reviews create noise, many reviews cite to other reviews as evidence, and a great number of them are mixing data from various parts of the body as well as *in vitro* and *in vivo* data, which increases the confusion. Finding real research papers on brain GCX topics may in many cases therefore not yet be possible, simply because that research has not yet been carried out and in part owing to technical difficulties.

We will now turn to the possible involvement of the GCX in neurodegenerative disease etiology. Noted with excitement is that on February 26, 2025, the first ever *Nature* article in this field was published entitled "*Glycocalyx dysregulation impairs blood–brain barrier in ageing and disease*" that will herein be briefly discussed ((Shi et al., 2025), Graphical Abstract sub-figures). With this study, it seems fair to say that research on the GCX may well be entering a Golden Age.

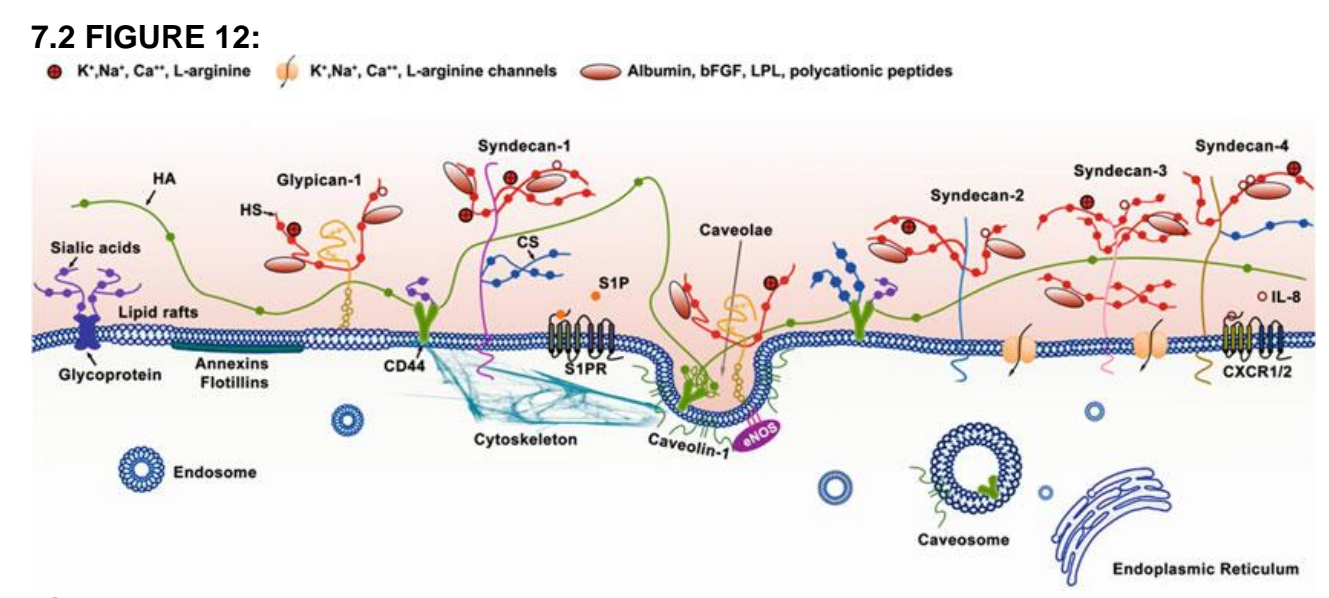


Figure 12. Structural components of the endothelial glycocalyx (ESG). The ESG is mainly located at the luminal side of vascular ECs although syndecan-4 is dominantly basal. The apical GAGs and associated proteins and ions are directly in contact with the bloodstream, and they transfer flow forces to the core proteins that transmit them to the cell. In addition to bound plasma components, the ESG is mainly composed of glycoproteins bearing acidic oligosaccharides and terminal sialic acids (SA); proteoglycans (PG), such as heparan sulfate proteoglycans (HSPGs, the Syndecan family and glypican-1); and GAG side chains. The predominant GAGs in ECs are heparan sulfate (HS), chondroitin sulfate (CS), and hyaluronic acid (hyaluronan, HA). HS and CS are attached to PGs. HA binds with receptor CD44. Membrane 'rafts' are more or less ordered

domains in the plasma membrane, classified as 'protein'- or 'lipid'- based. Syndecans (including syndecan-1, syndecan-2, syndecan-3, and syndecan-4) are single transmembrane domain proteins that interact with cytoskeleton (actin, in particular); they are localized in protein-based membrane rafts (e.g. caveolae). Glypican-1 is a membrane glycosylphosphatidylinositol (GPI)-anchored protein, which is localized in lipid rafts, as well as caveolae (Parton and del Pozo, 2013). Caveolin-1 anchors caveolae to the actin cytoskeleton and is important for plasma membrane shear stress mechanosensation that may mediate activation of eNOS and subsequent NO production. Lipid rafts are characterized by high translational mobility. Integrity of the actin cytoskeleton is essential for the immobility of caveolae. Syndecan-1 and CD44 interact with the cytoskeleton. Annexins and flotillins might be involved in the formation and function of caveolae. Some fraction of HA bound to CD44 are internalized into caveolae. The phosphorylation of caveolin-1, a protein responsible for maintaining the shape of caveolae, is induced in a HA-dependent manner, which might be involved in CD44caveolae-mediated endocytosis. It has been assumed that internalized caveolae fuse with caveosomes. Caveosomes play an important role in transcytosis of its contents such as albumin to other subcellular (nonlysosomal) compartments including the endoplasmic reticulum in ECs. Sphingosine-1-phosphate (S1P) protects the shedding of GCX and induces the synthesis of GCX that is required for mechanotransduction and cytokine response (i.e., IL-8/CXCR1/2- induced EC migration). (Figure adapted from (Zeng et al., 2018) and legend adapted from (Zeng and Tarbell, 2014; Zeng et al., 2018) and (Parton and del Pozo, 2013)).

7.3 STARLING'S EXPERIMENTS LEADING TO THE STARLING PRINCIPLE

Starling formulated the principle in qualitative terms following quantitative experiments using dogs. To start with, either isotonic saline solutions, or alternatively serum solutions, were injected into the connective tissue of one hind limb (the 'edematous leg'), whereas the other leg was used as a control (Starling, 1896). To investigate whether blood vessels could take up fluid, he would split blood in two portions, one for each leg. Then 12-25 times pass the same of each portion of blood through the same femoral artery, in either the injected or the control leg, and thereafter measured its volume and haemoglobin concentration upon collection from the venous side at the end of the 12-25 passes. Blood (and likewise fluid with serum) passed through the edematous leg was more dilute afterwards than blood passed through the control leg. In other experiments, where serum was injected into the connective tissue, there was no change in the composition of the blood afterwards.

The summary was that due to the high blood pressure in arteries, fluid is pressed out of vessel capillary walls into the interstitium. The fluid then returns from the interstits to the vessels on the venous side due to the lower blood pressure there, combined with the now relatively higher albumin concentration in the vessel, resulting in an increased oncotic pressure in the venous vessel compared with the arterial side.

To measure the oncotic pressure exerted by proteins, he designed an osmometer by measuring the pressure exerted over a semipermeable peritoneal membrane (coated with gelatine to make it more water tight but still water permeable) with on one side isotonic salt and blood plasma proteins (the serum) and on the other side isotonic salt only. He measured the blood plasma oncotic pressure to 30-40 mmHg, which took several days to equilibrate, and which is comparable with the measurements made today. He recognized this not to be a lot, but importantly of the same order of magnitude as the capillary blood pressure. In conclusion he writes: "...at any given time, there must be a balance between the hydrostatic pressure of the blood in the capillaries and the osmotic attraction of the blood for the surrounding fluids....Here then we have the balance of forces necessary to explain the accurate and speedy regulation of the quantity of circulating fluid", which is the Starling Principle stated in words, as we know it from textbooks ((Starling, 1896), p. 324); the principle listed as an equation was not published before around 1930 following further experiments by Landis and others. In addition, he was concerned about the lymphatic system as a possible error source in the fluid balance calculation, and aware that eventual excess fluid is transported away from the interstitial space through the lymphatic system and

back to the blood stream. In short, Starling's Principle states there is net filtration in the capillaries on the arterial side and nearly equal reabsorption on the venous side due to osmosis, and a minor fraction becomes lymph flow.

It seems likely that the Starling Principle has been so embraced through all these years, and still is, because of the easily understandable notion that a balance - an equilibrium - of two opposing forces regulates the fluid distribution.

Starling recognized that somehow blood vessels are permeable to protein, albeit not very much, which later has been described in mathematical terms with the walls osmotic reflection coefficient (σ) ranging between 0 and 1. Starling was puzzled concerning proteins and considered that to change their concentration they could move by crossing membranes through filtration or the cells could feed on them and the proteins would disappear.

Yet, he had no indication that the proteins were filtered and hypothesized that if proteins could be absorbed by ECs that could be a mechanism for transmembrane transport:"...a proof that proteids are absorbed in these situations would point to an active intervention of the endothelial cells in the process" (Starling (1896), p. 325).

Indeed, today we know proteins can be transported across the ECs through both transcytosis and paracellular transport.

Date: March 20, 2025.

Epilogue

Der Wanderer über dem Nebelmeer, (c1817) [Wanderer above the Sea of Fog] Caspar David Friedrich (1774 - 1840), Öl auf Leinwand 94.8cm x 74.8cm, Hamburger Kunsthalle, Deutschland.

Acknowledgements

Thanks to M. Lauritzen for proposing the theme and to N. Kutuzov and K. Kucharz for their interesting papers on the topic. Thanks to M. Hayden, R. Daneman and T. Woodcock for discussions and their interesting topical papers.

Typographical errors in Master's Thesis (April 22, 2025)

- p. 4, li 4 from bottom: perhaps this was due to different model...
- p. 4, Figure 3 legend:...narrow denser line about 15 nm from p (b points at this)...
- p. 6, li 7...shared by both the ECs and astrocytes. Then there may....
- p. 9, li 19 from bottom:.percentage area of total vessel lumen with GCX in brain capillaries.
- p. 10, Fig. 9(B) y-axis: % proportion of vessel lumen, y-axis is (nm) [and not (□m)]
- p. 26, 2. section:..in vivo studies for a long time, in part as it collapses...
- p.31-34: Figures numbered 20-22 should be numbered 21-23; also in the text.
- p. 34, li 6 from bottom:..mice that expressed the B3gnt3p enzyme behaved..[not C1galt1p]

List of permission licenses to reproduce figures shown herein

- Figure 1 From Essential Cell Biology, 5th edition, by Alberts et al. (2019), Fig. 11-33. Copyright 2019 by Bruce Alberts, Dennis Bray, Karen Hopkin, Alexander Johnson, the Estate of Julian Lewis, David Morgan, Martin Raff, Nicole Marie Odile Roberts, and Peter Walter. Licensed by W. W. Norton & Company.
- Figure 2 From Reily et al. (2019), Box 1 figure, licensed by Springer Nature.
- Figure 3 (left) from Hama (1960), Fig. 4, licensed by Rockefeller Institute Press; (right) from Luft (1971), Fig. 41, licensed by John Wiley and Sons.
- Figure 4 From Udan et al. (2013), Fig. 5, licensed by John Wiley and Sons.
- Figure 5 From Terstappen et al. (2021), Fig. 1, licensed by Springer Nature.
- Figure 6 From Vimptrup (1922), plate II, Fig. 5. Public Domain.
- Figure 7 From Galea (2021), Fig. 2, licensed by Creative Commons CC BY.
- Figure 8 From Daniele et al. (2021), licensed by Springer Nature.
- Figure 9 From (A, B) Ando et al. (2018), Fig. 1A, 2A, 2D, Supl. Fig. 2, licensed by Creative Commons CC BY; (C) from Kutuzov et al. (2018), Fig. 2B, licensed by PNAS standard terms.
- Figure 10 From (A) Ballinger et al. (2004), Fig. 1A, and (B) from Milusev et al. (2022), Fig. 1, licensed by Creative Commons CC BY.
- Figure 11 From (A) Becker et al. (2010), Fig. 6, licensed by Springer Nature; (B) from Dancy et al. (2024), Fig. 1, licensed by Creative Commons CC BY.
- Figure 12 From Zeng et al. (2018), Fig. 2, licensed by Springer Nature.
- Figure 13 From Ghitescu and Robert (2002), Fig. 6, licensed by John Wiley and Sons.
- Figure 14 From (A1, B1) Levick and Michel (2010), Fig. 2A, licensed by Oxford University Press; (A2, B2) from Alphonsus and Rodseth (2014), Fig. 1 and 2, licensed by John Wiley and Sons.
- Figure 15 From Machin et al. (2018), Fig. 4, licensed by The American Physiological Society.
- Figure 16 From Kutuzov et al. (2018), Fig. 2A-D, Fig. 4 A, C, Table 1, licensed by PNAS standard terms.
- Figure 17 From Pulgar (2018), Fig. 1, licensed by Creative Commons CC BY.
- Figure 18 From Schmidt et al. (2012), Fig. 1 A, B and Fig. 3 A, B, licensed by Springer Nature.
- Figure 19 From Schmidt et al. (2012), Supplementary Fig. 12, licensed by Springer Nature.
- Figure 20 From (A, C) Hayden (2023), Fig. 6C, D and Fig. 7 licensed by Creative Commons CC BY.; (B) from Erickson et al. (2023), Fig. 5B, licensed by Creative Commons CC BY.
- Figure 21 From Cruz-Hernandez et al. (2019), Fig. 6, licensed by Springer Nature.
- Figure 22 From Smyth et al. (2022), Fig. 6, licensed by Creative Commons CC BY.
- Figure 23 From Shi et al. (2025), Fig. 1 B-F, licensed by Creative Commons CC BY.
- Page 43 Der Wanderer über dem Nebelmeer, (c1817) by Caspar David Friedrich. Hamburger Kunsthalle, Germany, online objekt HK-5161 (BPK photo by Elke Walford). Public Domain.

Graphical Abstract (Cover, p. 1) shown hereunder, where the color marked boxes indicate the origin of the figure elements as follows:

(From open access Shi et al. (2025), Fig. 1a, Supplementary Fig. 1a-d, licensed by Creative Commons CC BY.
(—) From Cruz-Chu et al. (2014), Fig. 1, licensed by Elsevier.
(———	—) From Levick and Michel (2010), Fig. 2 A, licensed by Oxford University Press.
(—) From Cruz-Hernandez et al. (2019), Fig. 6, licensed by Springer Nature.

- () From Hayden (2023), Fig. 7, licensed by Creative Commons CC BY.
- () From Kucharz et al. (2022a), part of Fig. 1A, licensed by Springer Nature.
- (———) From Soliman et al., A guide for blood-brain barrier models, Fig. 3E, FEBS Lett (2024) licensed by John Wiley and Sons.

